

DISCLAIMER

This report was prepared as an account of work sponsored by an agency of the United States Government. Neither the United States Government nor any agency thereof, nor any of their employees, makes any warranty, express or implied, or assumes any legal liability or responsibility for the accuracy, completeness, or usefulness of any information, apparatus, product, or process disclosed, or represents that its use would not infringe privately owned rights. Reference herein to any specific commercial product, process, or service by trade name, trademark, manufacturer, or otherwise does not necessarily constitute or imply its endorsement, recommendation, or favoring by the United States Government or any agency thereof. The views and opinions of authors expressed herein do not necessarily state or reflect those of the United States Government or any agency thereof. Reference herein to any social initiative (including but not limited to Diversity, Equity, and Inclusion (DEI); Community Benefits Plans (CBP); Justice 40; etc.) is made by the Author independent of any current requirement by the United States Government and does not constitute or imply endorsement, recommendation, or support by the United States Government or any agency thereof.

SANDIA REPORT

SAND2025-12476

Printed October 2025

Sandia
National
Laboratories

Quantitative Risk Assessment for Fuel Cell Electric Bus Hydrogen Storage and Refueling Facility

Melissa S. Louie, Marina Miletic, and Brian D. Ehrhart

Prepared by
Sandia National Laboratories
Albuquerque, New Mexico
87185 and Livermore,
California 94550

Issued by Sandia National Laboratories, operated for the United States Department of Energy by National Technology & Engineering Solutions of Sandia, LLC.

NOTICE: This report was prepared as an account of work sponsored by an agency of the United States Government. Neither the United States Government, nor any agency thereof, nor any of their employees, nor any of their contractors, subcontractors, or their employees, make any warranty, express or implied, or assume any legal liability or responsibility for the accuracy, completeness, or usefulness of any information, apparatus, product, or process disclosed, or represent that its use would not infringe privately owned rights. Reference herein to any specific commercial product, process, or service by trade name, trademark, manufacturer, or otherwise, does not necessarily constitute or imply its endorsement, recommendation, or favoring by the United States Government, any agency thereof, or any of their contractors or subcontractors. The views and opinions expressed herein do not necessarily state or reflect those of the United States Government, any agency thereof, or any of their contractors.

Printed in the United States of America. This report has been reproduced directly from the best available copy.

Available to DOE and DOE contractors from

U.S. Department of Energy
Office of Scientific and Technical Information
P.O. Box 62
Oak Ridge, TN 37831

Telephone: (865) 576-8401
Facsimile: (865) 576-5728
E-Mail: reports@osti.gov
Online ordering: <http://www.osti.gov/scitech>

Available to the public from

U.S. Department of Commerce
National Technical Information Service
5301 Shawnee Rd
Alexandria, VA 22312

Telephone: (800) 553-6847
Facsimile: (703) 605-6900
E-Mail: orders@ntis.gov
Online order: <https://classic.ntis.gov/help/order-methods/>



ABSTRACT

Hydrogen-powered bus fleet deployment is being explored in several municipalities across the United States, and it is important to understand potential risks and safety implications of regular hydrogen fuel cell electric bus (FCEB) operations such as refueling. We conducted a quantitative risk assessment for the hydrogen production, storage, compression, and refueling operations for a generic FCEB bus fleet, focusing on the risk of annual frequency of fatality due to potential hydrogen leaks, for a person in the vicinity of the facility. We discuss relative risk contributions by component and physical outcome (i.e., jet fires and explosions) and provide insight into appropriate hazard and risk prevention and mitigation related to design, operations, and personnel training. We also tabulate component leak frequency data and outcome probabilities through customized fault trees and event sequence diagrams, respectively, to demonstrate how to determine appropriate data and inputs for other/future risk assessments.

ACKNOWLEDGEMENTS

This material is based upon work supported by the U.S. Department of Energy's Office of Energy Efficiency and Renewable Energy (EERE) under the Hydrogen and Fuel Cell Technologies Office (HFTO). This work was performed as part of a cooperative research and development agreement (CRADA) with the Pacific Northwest National Laboratory (PNNL), and the Port of Portland/Portland International Airport (PDX). The authors thank Dusty Brooks, Chris LaFleur, and Kristin Hertz from Sandia National Laboratories and Arun Veeramany from the Pacific Northwest National Laboratory for their technical reviews of this work.

EXECUTIVE SUMMARY

It is necessary to understand the safety implications and risk mitigation options for fuel cell electric bus fleet deployment, especially for related facilities responsible for operations such as production, storage, compression, and dispensing of hydrogen for use by the buses. In this report, we present a quantitative risk assessment for a potential fuel cell electric bus fleet that was motivated by efforts to improve resilience at the Portland International Airport but can be applicable to a range of hydrogen case studies and use cases.

We estimated risk for a facility that produces, stores, compresses, and dispenses hydrogen for the fleet of buses, with a focus on individual risk to people in terms of annual frequency of fatality. We considered the frequency of hydrogen leaks that could result in harmful physical outcomes like jet fires or explosions, and the consequences of those outcomes for people. We created customized fault trees to calculate the frequencies of different sizes of leaks and event sequence diagrams to calculate ignition probabilities for the various leak sizes. We also leveraged the HyRAM+ toolkit to use these inputs to calculate overall risk for the facility, which we separated into one section responsible for producing, storing, and compressing hydrogen, and one section responsible for dispensing the hydrogen to the buses.

We found that the dispensing area seemed to have a higher risk than the production/storage/compression area of the facility, largely because of the inclusion of a component with a high leak frequency (the heat exchanger used to cool the hydrogen before entering the vehicle, to prevent overheating and expansion of hydrogen in the onboard tank). For the example production and refueling facility we evaluated and the data we used for the analysis, the leak frequency had a larger impact on the risk differences between the two sections on the facility, compared to the physical outcome consequence, which was slightly different due to the varying fuel conditions, but not substantially different.

Actions can be taken to prevent these hazards (e.g., lowering leak frequencies in system components) or to mitigate the consequences if they do occur (e.g., installing barriers to protect people if ignition events occur). The choice of which actions to take depends not only on safety considerations but also on space, time, staffing, feasibility, and financial constraints. Therefore, the quantitative risk assessment approach can help understand relative risk contributions from different components, leak sizes, consequences, and human actions, to prioritize risk reduction strategies and balance these parameters.

The outcomes of this report may be useful for a variety of stakeholders working in the hydrogen, transportation, vehicle, and aviation sector, including those responsible for aspects like facility design, operations, and regulations. There is not a single value of risk that determines whether a hypothetical system is “safe” or not. The insights about risk mitigations may be leveraged, and the quantitative risk assessment approach can be applied to other case studies to understand risk priorities and contributions specific to different FCEB and hydrogen facility uses.

CONTENTS

Abstract	3
Acknowledgements.....	4
Executive Summary.....	5
Acronyms and Terms.....	10
1. Introduction.....	11
1.1. Motivation	11
1.2. Hydrogen Fuel Cell Electric Bus Selection	11
1.3. Fueling Station Design.....	11
2. Methods.....	13
2.1. System Setup.....	13
2.2. Component Leak Frequencies.....	15
2.3. Model Inputs.....	15
3. Results and Discussion.....	18
3.1. Leak and Ignition Frequencies.....	18
3.2. Production, Compression, and Storage Area Risk.....	21
3.3. Dispenser Area Risk.....	22
3.4. Risk Reduction Through Prevention and Mitigation.....	23
4. Conclusion.....	26
References.....	27
Appendix A. Fault and Event Trees Used for QRA	29
A.1. Fault Trees.....	29
A.1.1. Production, Storage, and Compression Area	29
A.1.2. Dispensing Area.....	32
A.1.3. Fault Tree Data.....	37
A.2. Event Sequence Diagram	38
Appendix B. Hazard Contours.....	41
B.1. Jet Fire Consequences.....	41
B.2. Explosion Consequences.....	45
Distribution.....	47

LIST OF FIGURES

Figure 2-1. Generic hydrogen refueling station setup. Not to scale.....	13
Figure 2-2. Generic schematic of production, compression, and storage system.....	14
Figure 2-3. Generic schematic of dispenser system.....	14
Figure 3-1. Example generic fault tree for per-component annual frequency of leaks from 0.01% leak in the production, storage, and compression area. Same image as shown in Figure A-1.....	18
Figure 3-2. Example generic fault tree for per-component annual frequency of leaks from 0.01% leak in the dispensing area. Same image as shown in Figure A-6.....	19
Figure 3-3. Example generic fault tree for full-bore leak frequencies in the dispensing area, including per-component annual frequency of leaks and dispenser-specific accidents and per-refueling shutdown failure probabilities. Same image as shown in Figure A-10.....	20
Figure 3-4. a) Risk based on distance from a leak, for a person assumed to be directly in front of the leak and b) risk based on location in relation to a leak for the production, compression, and storage area of the facility	21
Figure 3-5. a) Risk based on distance from a leak, for a person assumed to be directly in front of the leak and b) risk based on location in relation to a leak for the dispenser area of the facility. 23	23
Figure A-1. Generic fault tree for 0.01% leak from the storage and compression area. Provided numbers are per-component median annual leak frequencies for a single instance of each included component.....	29
Figure A-2. Generic fault tree for 0.1% leak from the storage and compression area. Provided numbers are per-component median annual leak frequencies for a single instance of each included component.....	30
Figure A-3. Generic fault tree for 1% leak from the storage and compression area. Provided numbers are per-component median annual leak frequencies for a single instance of each included component.....	30
Figure A-4. Generic fault tree for 10% leak from the storage and compression area. Provided numbers are per-component median annual leak frequencies for a single instance of each included component.....	31
Figure A-5. Generic fault tree for 100% leak from the storage and compression area. Provided numbers are per-component median annual leak frequencies for a single instance of each included component.....	31
Figure A-6. Generic fault tree for 0.01% leak from the dispensing area. Provided numbers are per-component median annual leak frequencies for a single instance of each included component. * indicates that the frequencies below were multiplied by the assumed total refueling time per year.....	32
Figure A-7. Generic fault tree for 0.1% leak from the dispensing area. Provided numbers are per-component median annual leak frequencies for a single instance of each included component. * indicates that the frequencies below were multiplied by the assumed total refueling time per year.....	33
Figure A-8. Generic fault tree for 1% leak from the dispensing area. Provided numbers are per-component median annual leak frequencies for a single instance of each included component. * indicates that the frequencies below were multiplied by the assumed total refueling time per year.....	34
Figure A-9. Generic fault tree for 10% leak from the dispensing area. Provided numbers are per-component median annual leak frequencies for a single instance of each included component. * indicates that the frequencies below were multiplied by the assumed total refueling time per year.....	35

Figure A-10. Generic fault tree for 100% leak from the dispensing area. Provided numbers are per-component median annual leak frequencies for a single instance of each included component except for **, which are leak probabilities per refueling. * indicates that the frequencies below were multiplied by the assumed total refueling time per year.	36
Figure A-11. Event sequence diagram with probabilities (rectangles) and annual frequencies (non-rectangles) for a) 0.01%, b) 0.1%, c) 1%, d) 10%, and e) 100% leak for the production, compression, and storage area.....	39
Figure A-12. Event sequence diagram with probabilities (rectangles) and annual frequencies (non-rectangles) for a) 0.01%, b) 0.1%, c) 1%, d) 10%, and e) 100% leak from dispenser area.	40
Figure B-13. Heat flux contours from a jet fire from a) 0.01%, b) 0.1%, c) 1%, d) 10%, and e) 100% leak directed in the +x direction, for components before the chiller carrying hydrogen at 20°C (68°F) and 900 bar (13,053 psi). x values are in the direction of the leak, z values are perpendicular to the leak, and y values correspond to height.	41
Figure B-14. Heat flux contours from a jet fire from a) 0.01%, b) 0.1%, c) 1%, d) 10%, and e) 100% leak directed in the +x direction, for components after the chiller carrying hydrogen at -40°C (-40°F) and 700 bar (10,153 psi). x values are in the direction of the leak, z values are perpendicular to the leak, and y values correspond to height.	42
Figure B-15. Temperature contours from a jet fire from a) 0.01%, b) 0.1%, c) 1%, d) 10%, and e) 100% leak directed in the +x direction, for components before the chiller carrying hydrogen at 20°C (68°F) and 900 bar (13,053 psi).....	43
Figure B-16. Temperature contours from a jet fire from a) 0.01%, b) 0.1%, c) 1%, d) 10%, and e) 100% leak directed in the +x direction, for components after the chiller carrying hydrogen at -40°C (-40°F) and 700 bar (10,153 psi).....	44
Figure B-17. Overpressure contours from an explosive event from a) 0.01%, b) 0.1%, c) 1%, d) 10%, and e) 100% leak directed in the +x direction, for components before the chiller carrying hydrogen at 20°C (68°F) and 900 bar (13,053 psi). x values are in the direction of the leak, z values are perpendicular to the leak, and y values correspond to height.	45
Figure B-18. Overpressure contours from an explosive event from a) 0.01%, b) 0.1%, c) 1%, d) 10%, and e) 100% leak directed in the +x direction, for components after the chiller carrying hydrogen at -40°C (-40°F) and 700 bar (10,153 psi). x values are in the direction of the leak, z values are perpendicular to the leak, and y values correspond to height.	46

LIST OF TABLES

Table 2-1. Component Counts.	16
Table 3-1. Priorities for Consequence and Risk Mitigation Actions	24
Table A-1. Component Annual Median Operational Leak Frequencies by Leak Size for Components in Gaseous Hydrogen Systems.	37
Table A-2. Dispenser-Specific Median Leak Probabilities per Refueling.	38

This page left blank

ACRONYMS AND TERMS

Acronym/Term	Definition
ANSI	American National Standards Institute
API	American Petroleum Institute
CFR	Code of Federal Regulations
CGA	Compressed Gas Association
GH2	gaseous hydrogen
HPIT	hydrogen powered industrial trucks
ISO	International Organization for Standardization
LH2	liquid hydrogen
LPG	liquefied petroleum gas
MAQ	maximum allowable quantity
NHTSA	National Highway Traffic Safety Administration
NFPA	National Fire Protection Association
OSHA	Occupational Safety and Health Administration
SAE	Society of Automotive Engineers
SCF	standard cubic feet
TPRD	thermally activated pressure relief device

1. INTRODUCTION

Hydrogen is a potential alternative to diesel fuel for bus and mass transit applications. Therefore, it is valuable to understand the potential hazards and risks in the operation of these vehicles so mitigation actions can be taken at the facility level; the regulatory landscape, such as mandated requirements or recommended practices, can also be risk-based or risk-informed. In this report, we present results of a quantitative risk assessment (QRA) for the refueling station of a fuel cell electric bus (FCEB) to understand the components, leak sizes, and hazards of highest risk. This research can inform adoption of FCEBs for airport facility decision makers, engineers, designers, and regulators.

1.1. Motivation

The Portland International Airport (PDX), located in Oregon, is a civil-military airport that serves hundreds of flights per day and millions of passengers per year [1]. Recently, decision-makers at the airport have been working on efforts to improve resilience of PDX operations through the transition of their parking shuttle fleet from natural gas vehicles to hydrogen-powered FCEBs [2]. A major motivation for this initiative is the high potential for the occurrence of a high-intensity earthquake along the Cascadia Subduction Zone in Oregon within the next several decades, which could cause extensive damage to the built infrastructure of PDX [3]. Having a hydrogen FCEB fleet available onsite could provide a portable backup source of power for critical services at the airport in the event of a large seismic event and subsequent power outages, since fuel cells produce electricity [2], [4]. Understanding the overall risks of this technology adoption during everyday usage is important for safe design and operation.

While this study was initiated for this specific purpose, the QRA is not specific to the case study; it is generic, and the insights can be applied to other locations and hydrogen bus fleet applications.

1.2. Hydrogen Fuel Cell Electric Bus Selection

To perform analysis of hazards and risk, and to assess the viability of emergency power generation, it is necessary to know the specifications of the fuel cell electric buses that would be deployed if this type of vehicle were to be adopted for passenger transit at PDX. The QRA in this report is based on a 24-bus fleet for ground transport. After correspondence with Port of Portland personnel, the Xcelsior Charge FC New Flyer 40' hydrogen fuel cell electric bus was chosen as a representative vehicle to use in our analysis [5]. This bus model can carry up to 82 people (40 seated, 42 standing). Hydrogen tanks and batteries are mounted on the top of the vehicle. Tanks have a 37.5 kg of hydrogen base storage capacity and refueling should take between 6-10 minutes. The buses also have a net power rating of 100 kW.

This selection by no means implies that these buses will be selected for use at PDX or any other airport facility. The selection of these buses was performed strictly for the purpose of developing a more detailed analysis based on realistic vehicle specifications.

1.3. Fueling Station Design

To aid in performing quantitative and qualitative risk assessments, we selected a gaseous hydrogen station design described in literature with a capacity of 4186 kg/day. [6] After evaluating the upfront and ongoing/operational costs of different designs, we chose Case #2 from the *Reference Station Design for Heavy-Duty Vehicles* report from 2023 and adopted it for use for hydrogen fuel cell electric buses [6]. This design had the lowest combined capital and ongoing costs after 2 years, and the

lowest operational cost of all the designs presented. It also features onsite hydrogen generation, eliminating the need for hydrogen delivery. This aspect could be especially useful after an earthquake, when delivery of hydrogen, diesel, or other fuel may be infeasible, especially if the system itself is adequately hardened against seismic activity and is able to continue functioning after the event.

This station design assumes an approximate 20,000 ft² (1,858 m²) footprint for on-site production and dispensing of 750 bar -40°C gaseous hydrogen. This design involves hydrogen formation via electrolysis, performed on-site and during off-peak hours when electricity is cheaper. This process includes an electrolyzer unit which creates hydrogen from water and electricity, after which the hydrogen is sent to 100 bar storage tanks, followed by two stage compression which yields 940 bar hydrogen, which is then sent to a heat exchanger for cooling to -40°C, after which it is sent through a fuel dispenser which supplies the FCEBs. Though only 900 kg/day of hydrogen is needed to fuel the operation of this FCEB fleet, this process can generate 4186 kg/day. Because hydrogen generation does not need to occur continuously, this process can be stopped once its maximum capacity is reached. For example, if a 7-day contingency is desired, 6300 kg of gaseous hydrogen would need to be stored on site, which would require 34,980 gallons or 132.4 m³ of storage. The software Hydrogen Plus Other Alternative Fuels Risk Assessment Models (HyRAM+) v5.1 was used to calculate this volume of gaseous hydrogen based on 25°C and 940 bar conditions [7].

The design of the station in this report is a hypothetical example of a facility serving an FCEB fleet, and we do not intend to imply a recommendation or that such a station is superior and should be adopted over others. This station was selected in part because it was a generic, supplier-agnostic design with available specification information which could aid in risk assessment. The outcomes of this QRA are valuable because they bring attention to general risks that may be similar across many different facility designs, and because we demonstrate how to use a QRA, and which aspects may be helpful to consider when setting up system design and operation protocols.

2. METHODS

2.1. System Setup

We used HyRAM+ v5.1 to conduct a QRA for the bus refueling station. For the example assessment in this report, it was assumed that the area of the plant containing the production, compression, and storage equipment is enclosed by a fire and blast wall. Thus, two separate risk calculations were performed, one for the hydrogen production, compression, and storage area, and one for the hydrogen dispensing area. It was assumed that the hydrogen would be delivered from the production area to the dispensing area via a piping network in a trench covered by grates which allow for ventilation and easy access for maintenance and repair. Since the piping in the trench is open to the outside air, the piping in the trench was included in the QRA for the dispensing area. Figure 2-1 shows a mockup of the general setup of the hydrogen bus refueling station.

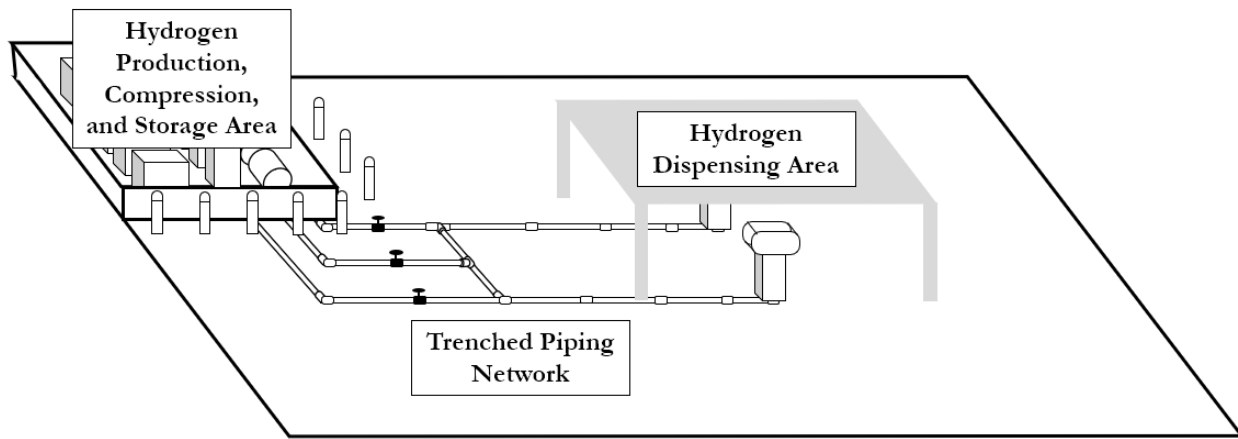


Figure 2-1. Generic hydrogen refueling station setup. Not to scale.

A more detailed schematic of the setup within the hydrogen production, compression, and storage enclosure is provided in Figure 2-2. First, hydrogen is produced by the electrolyzer. It is compressed and stored at multiple storage pressures. When a vehicle is present at the refueling station and there is demand at the dispenser, a valve downstream of the storage tanks opens, hydrogen is sent through a filter followed by a chiller to ensure that it is delivered at -40°C to prevent excessive increase in temperature during expansion in the tank of the vehicle. During refueling, both high-pressure and medium-pressure hydrogen is dispensed depending on the state of fill of the onboard tank and the required pressure differential. The cascading pressure system for the tanks is based on work by Caponi et al. [8].

The electrolyzer is not included in the QRA due to the lack of available electrolyzer leak data. The electrolyzer can be assumed to also be isolated by a fire/blast wall from the other components and from the area in which people would be present on a regular basis. If this is not done, then the risk calculated for this portion of the system may be an under-estimate.

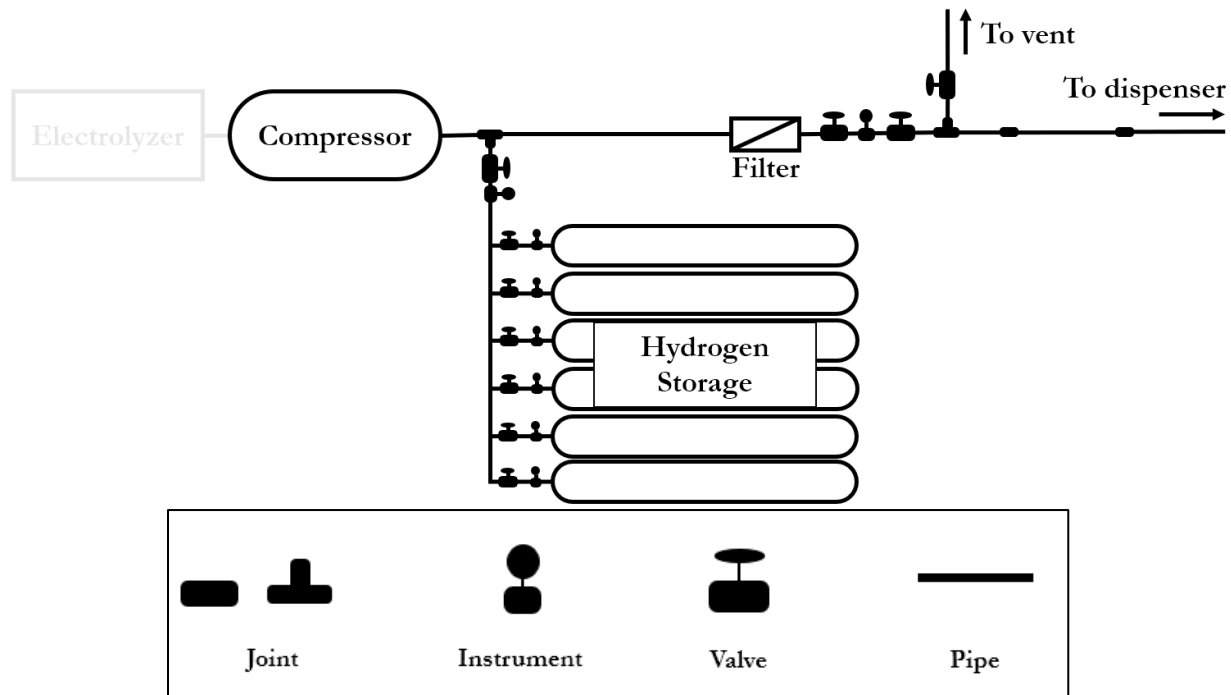


Figure 2-2. Generic schematic of production, compression, and storage system.

The schematic for the dispenser is provided in Figure 2-3. The dispenser QRA includes the components in the trench as well as the dispenser. The trench contains piping with joints and valves which carry the compressed hydrogen from the production/compression/storage area to the dispenser. The dispenser itself includes hoses, flowrate instrumentation, the breakaway, and the nozzle. The breakaway is the component that is designed to break off in the event of an accidental vehicle drive-off during refueling. When this occurs, an automatic shutoff valve stops the flow of hydrogen.

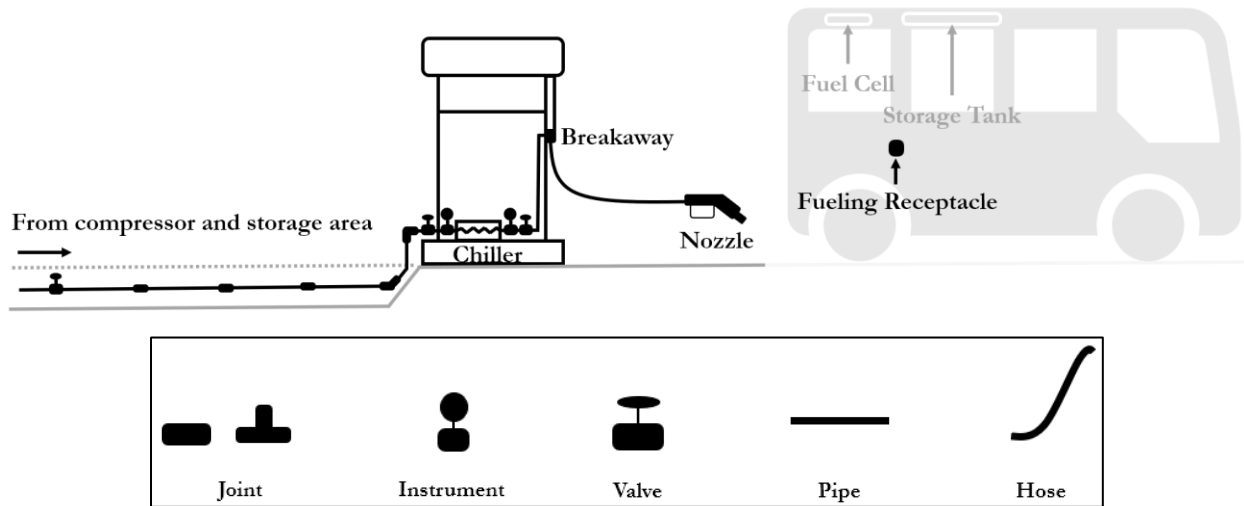


Figure 2-3. Generic schematic of dispenser system.

The QRA for the dispenser area also includes the fueling receptacle, which is the component onboard the FCEB that is connected to the nozzle of the dispenser hose during refueling. A more

extensive QRA could also include other hydrogen-containing components onboard the vehicle, such as the storage tank or the fuel cell, but, in the absence of leak frequency data for these types of components, we did not include them in this study. A vehicle-specific QRA would also be useful to consider the risks during operation, not only during refueling. As such, this QRA could be considered limited to the contribution of the refueling station itself, rather than an estimate of total possible risk.

The schematics presented above are all generic, meaning they show the overall layout for the hydrogen bus refueling station, but QRA inputs such as component counts may vary from what is pictured. The reference station design includes multiple compressors, high- and low-pressure storage vessels, and chillers, as well as multiple dispensers and their associated components [6]. This is generally not representative of most gaseous refueling stations which usually have fewer components because they may not have on-site off-peak hydrogen production using electrolyzers and low-pressure storage.

2.2. Component Leak Frequencies

We created customized fault trees to visually show the overall annual leak frequencies of leaks of five different sizes (0.01%, 0.1%, 1%, 10%, and 100% of the interconnecting piping cross-sectional area) and event sequence diagrams to calculate ignition probabilities, given these leak sizes. The leaks are assumed to occur at the connection between components. The data are taken from HyRAM+ v5.1 [7] except for filter data, which was taken from a report by Brooks et. al. [9]. While the leak data are best described by distributions, median values are provided in the fault trees in this analysis as a best estimate of central tendency.

It should be noted that the component fault trees we generated are not currently comprehensive of all failures that could occur for the included components, particularly for tanks or vessels. For example, there is likely to be a thermal pressure relief device (TPRD) on the vessel that can release hydrogen if overheating and overpressurization occur; while this event would represent the system functioning properly, it still indicates a potentially hazardous release of hydrogen and should be considered. The TPRD release is not included as a tank failure in these fault trees due to a scarcity of available frequency data. Similarly, tank rupture due to, for example, overheating and overpressurization and failure of the TPRD, is another important failure mechanism of tanks that could not be included in this fault tree because relevant data were not available.

We also included dispenser-specific failures in the fault tree for the hydrogen dispensing section of the facility. For these failures, we also used data from HyRAM+ v5.1 [7], which assumes that dispenser-specific failures are always full-bore leaks, or leaks with an area of 100% of the cross-sectional area of the facility's interconnecting piping.

2.3. Model Inputs

The component count list used for the QRA is shown in the following table. Note that the component counts in the table do not exactly reflect the schematics shown previously, because the schematics for the station design are not sufficiently detailed to include component counts for equipment like joints, instruments, valves, and pipes. The component counts were developed using insight from various hydrogen storage and refueling facility designs, including resources from Caponi et al. [8] and the Hyfindr project [10], [11].

Table 2-1. Component Counts.

Component	Count in Production, Compression, and Storage Area	Count in Dispenser Area
Compressor	1	0
Storage Tank	6	0
Filter	1	0
Chiller	0	1
Joint	16	9
Valve	8	4
Pipe ¹	20	50
Instrument	8	3
Breakaway	0	1
Hose	0	1
Nozzle	0	1
Receptacle (on vehicle)	0	1

The temperature and pressure for the production, compression, and storage area were set to 20°C (68°F) and 900 bar (13,053 psi). For the dispenser area, the temperature and pressure were set to 20°C (68°F) and 900 bar (13,053 psi) for components before the chiller, and -40°C (-40°F) and 700 bar (10,152 psi) for the chiller and subsequent components. The components before the chiller at the higher temperature and pressure consisted of 49 pipes, 3 valves, 8 joints, and 2 instruments, while the components at the lower temperature and pressure consisted of 1 pipe, 1 valve, 1 joint, 1 instrument, 1 chiller, 1 breakaway, 1 hose, 1 nozzle, and 1 on-vehicle receptacle. For simplicity, we assumed all components and interconnecting piping in each section had the same pipe diameter, with an inner diameter of 7.94 mm (5/16").

The risk was calculated as an individual annual frequency of fatality. This quantification was based on the Eisenberg probit model for human harm from radiative heat flux that would be emitted from a jet fire and the probit model for head impact resulting in fatality from the overpressure and impulse from an explosive event [12], [13], [14].

The HyRAM+ default inputs for the QRA were also used for the remainder of the inputs [1]. The relative humidity was 0.89, the discharge coefficient was 1, the probability of detection and isolation of a leak before any consequential events could occur was 0.9, the Bauwens-Strehlow-Tang overpressure method was used with a flame speed of Mach 0.35 to compute overpressure characteristics, and the HyRAM+ defaults for hydrogen ignition frequencies were used. Additionally, for conservatism and simplicity, the leak was assumed to have a fixed horizontal angle, with the leak assumed to be pointed directly at the person for the 1D results.

¹ Each pipe corresponds to a 1-m length of piping [7].

In HyRAM+ and this report, overall risk is the sum of the risk for each leak size. The risk of each leak size is quantified as the sum of risk from each potential outcome (jet fire or explosion); each of these risks is calculated as the product of the frequency and consequence of the outcome [7].

The frequency is calculated using the frequency of each size leak, based on generic component data discussed in Section A.1 and the default HyRAM+ event sequence diagram [7]. The calculated outcome frequencies, which aggregate data for all the components in each system, are provided in event sequence diagrams in Figure A-11 and Figure A-12.

The consequence is calculated using physics modeling of heat flux for jet fires and overpressure and impulse for explosions, as well as probit models that convert exposures to these physical outcomes to probabilities of fatality. The physical outcomes are shown in Appendix B as heat flux and temperature contours for the associated jet fires, and overpressure contours for the associated explosive events. The main characteristics of the jet fire plots are that they are directional – areas behind the leak or in locations not in the direct line of the leak tend to experience lower heat fluxes – and that the area affected by a jet flame increases with increasing leak size. The overpressure hazards tend to have more of a radial profile, so the experience of high overpressures depends mostly on the distance from the leak point in general and not on the direction in which the leak is pointing. The area affected by potentially harmful overpressures also increases as the leak size gets larger.

The results of this risk assessment are meant to demonstrate the methodology of conducting a QRA for a hydrogen system, with some considerations specific to a refueling facility. However, it is important to note that the results are not meant to reflect absolute risk numbers for use in specific cases or systems, especially because the selected inputs were assumed for this reference system in the absence of more site-relevant data. For example, the 0.9 probability of leak detection and isolation was an estimate, but, in a real system, it could be higher or lower based on aspects like the quality and placement of the sensors, and the shutdown controls included in the system. The data used for component leak frequencies, dispenser leak probabilities, and ignition probabilities is highly uncertain, partially because of the lack of hydrogen-specific industry leak data [9], [15]. The value of this QRA, besides the demonstration of the methodology, is also in showing how QRA results may be interpreted and used to determine concrete preventive and mitigative actions that can be taken by owner-operators to improve system safety.

3. RESULTS AND DISCUSSION

3.1. Leak and Ignition Frequencies

We developed fault trees to calculate overall frequencies of each size leak for both the production, compression, and storage area and for the dispensing area. Figure 3-1 shows one example of a fault tree, where the displayed numbers reflect per-component annual leak frequencies. The format of the fault trees for the remaining leak sizes in the production, compression, and storage area follows the same format as the one shown below, with the listed per-component leak frequencies. Thus, to calculate overall leak frequencies, each component leak frequency was multiplied by the number of that type of component. The full set of fault trees for this part of the facility is provided in Appendix A.1.1.

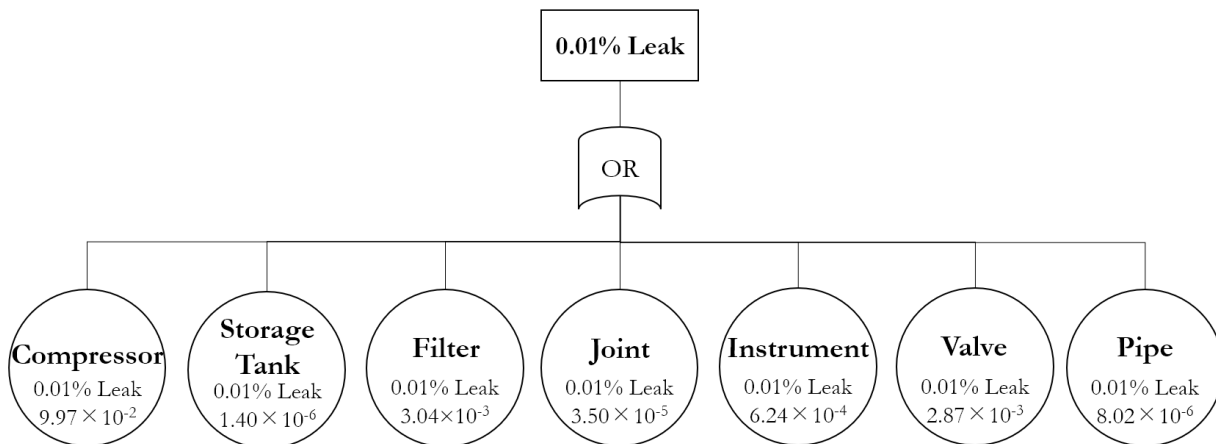


Figure 3-1. Example generic fault tree for per-component annual frequency of leaks from 0.01% leak in the production, storage, and compression area. Same image as shown in Figure A-1.

Both per-component leak frequencies and overall leak frequencies for a type of component can be useful information for the facility owner-operator; the number of components impacts the overall system leak frequency contributions from each component type. For example, for the production, storage, and compression section, we assumed that there was 1 filter and 8 instruments. By individual component, each filter has a higher 0.01% leak frequency than each instrument (3.04×10^{-3} per year for filters, compared to 6.24×10^{-4} per year for instruments). However, altogether, the overall 0.01% leak frequency for instruments in the system is 4.99×10^{-3} per year. This distinction indicates that the filter may be expected to have more 0.01% leaks than each instrument, but that, overall, the system has a higher frequency of having a 0.01% instrument leak somewhere in this part of the facility than a 0.01% filter leak. Both pieces of information can be informative to owner-operators when determining activities such as leak monitoring/sensing locations within the facility, and inspection or maintenance.

We also generated leak frequency fault trees for the dispenser area. The full set of fault trees for the dispensing area is included in Section A.1.2. For non-full-bore leaks (those that are 0.01%, 0.1%, 1%, and 10% of the cross-sectional area of interconnecting piping), the fault trees are similar to the ones for the production, storage, and compression area; each component is estimated to have a certain annual leak frequency, and the sum of all the leak frequencies for all system components is the overall system leak frequency.

As discussed previously, the data for these fault trees were taken from HyRAM+ v5.1 and the report by Brooks et al. [9]. Besides the filter data in the latter source, the component leak frequencies were sourced from a paper by LaChance et al., which in turn lists several sources from which raw data was taken [15]. The generic data sources themselves do not specify whether the annual leak frequencies are representative for continuously operational equipment or if they may include intermittencies due to routine maintenance, forced shutdown, or other circumstances. This information about the data is important because the components in the dispenser section of the facility are assumed to only be filled to the refueling pressure with hydrogen when a vehicle is present and refueling is actively taking place. Thus, using data for continuously operating equipment could lead to an overestimate of risk, especially if the facility has a large amount of downtime. The various data sources cited by LaChance et al. include facilities for a wide range of industries like chemical processing plants, onshore and offshore hydrocarbon facilities, pipelines, and nuclear power plants. With this limited information, the assumption was made that these types of facilities would generally be run continuously, and that any intermittencies due to maintenance or accidents would not be akin to the regular intermittency experienced by a refueling station. Therefore, a factor or prerequisite that the vehicle is at the refueling station for those frequencies to be applicable was added to the fault trees for the dispenser section. This factor is denoted by an oval titled “Presence of Vehicle at Refueling Station*.”

For this assessment, the hydrogen bus fleet at PDX is supposed to include 24 New Flyer xcelsoir Charge FC buses [5], and each is expected to undergo one refueling per day. Assuming the use of a single dispenser at the station and an upper limit of refueling time of 10 minutes per bus, there will be 24 refuelings per day for a total of 240 refueling minutes per day. Over the course of the year, there will be 8760 refuelings and 87,600 minutes of refueling; thus, in terms of time, the dispenser and its associated equipment will be pressurized with hydrogen for around 16.7% of the year. For all the component branches of the dispenser fault trees (“Hose”, “Breakaway”, “Nozzle”, “Joint”, “Instrument”, “Valve”, and “Pipe”), the number in the branch was multiplied by 16.7%.

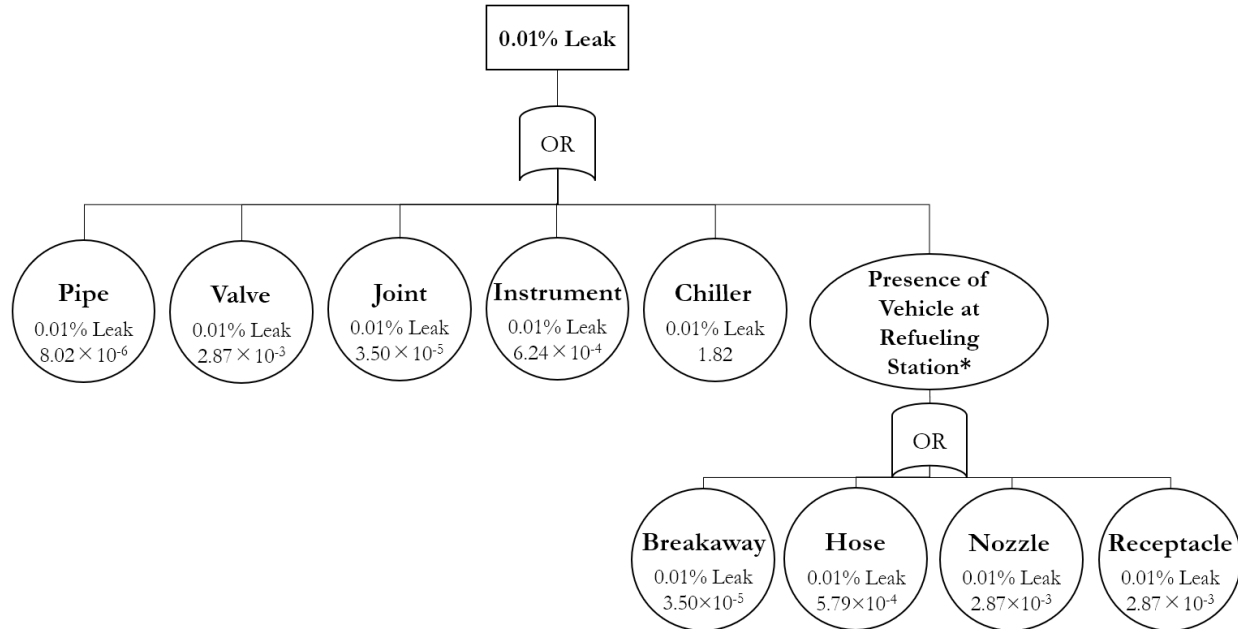


Figure 3-2. Example generic fault tree for per-component annual frequency of leaks from 0.01% leak in the dispensing area. Same image as shown in Figure A-6.

For the full-bore leaks in the dispensing section, as described in Section 2.2, the possibility of dispenser-specific leaks was also included. These data were included as median estimated leak probabilities per refueling event rather than frequencies per year; they were multiplied by the total estimated refueling time (based on the fleet number and expected fueling frequency and time).

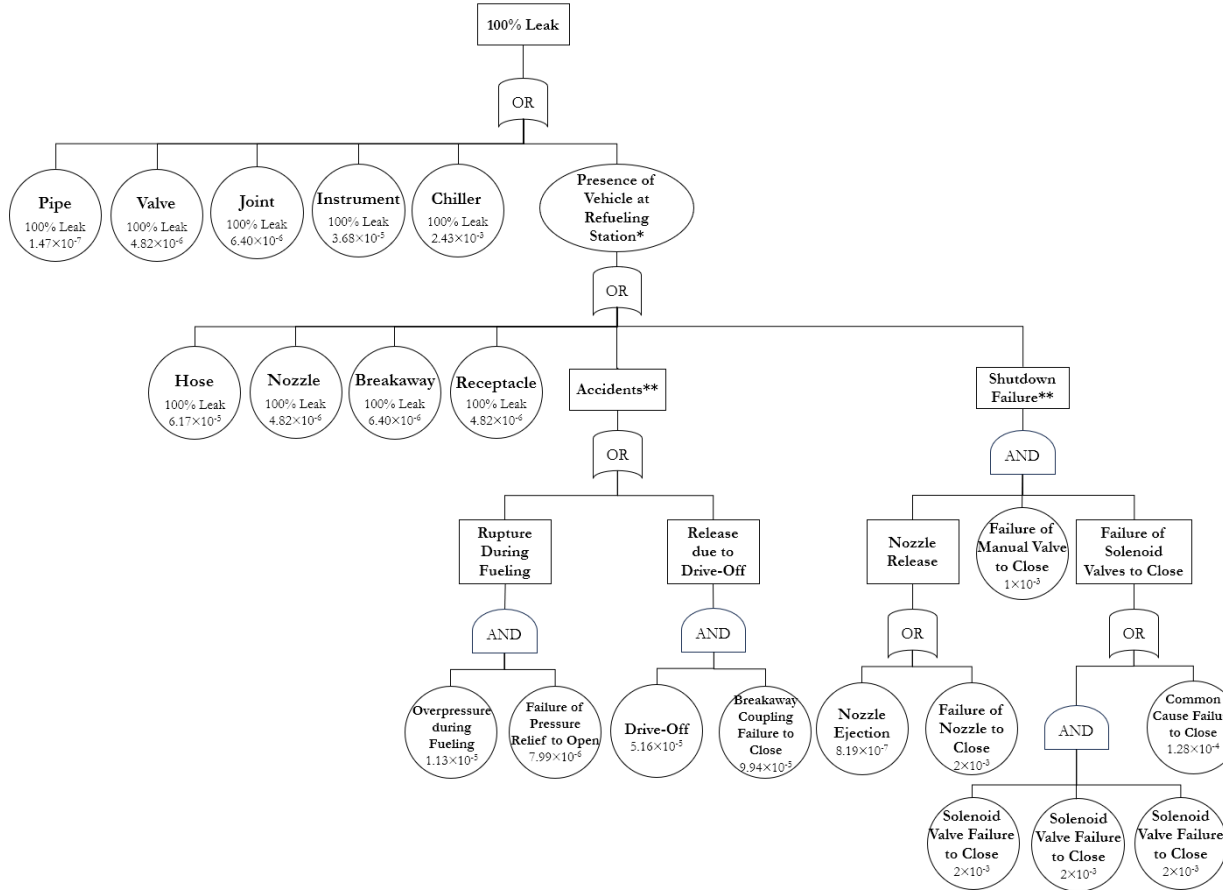


Figure 3-3. Example generic fault tree for full-bore leak frequencies in the dispensing area, including per-component annual frequency of leaks and dispenser-specific accidents and per-refueling shutdown failure probabilities. Same image as shown in Figure A-10.

In Figure 3-3 above, there are two added branches for Accidents and Shutdown Failures specific to the dispenser equipment and function. These two branches are labeled ** because the numbers provided underneath them indicate probabilities of failure per refueling instance, which is a different unit from the annual frequencies of failure provided for the component leaks. Therefore, the numbers under the branches for accidents and shutdown failures should be multiplied by the number of refueling instances per year, contrary to the component failure frequencies, which should be multiplied by the percentage of the year, timewise, for which refueling is expected to take place. The Figure 3-3 fault tree was developed based on a dispenser configuration where a shutdown failure (shown by the rightmost branch on the diagram) is caused by three events: the release of the dispenser nozzle, the failure of the manual valve to close, and the failure of all three solenoid valves to close. For the solenoid valve failures, there can either be an independent and simultaneous failure of all three solenoid valves (for example, due to rust or breakage of the valves), or there can be a single event that affects all the valves (for example, an electrical malfunction or catastrophic impact

affecting all the solenoid valves at once). Either of these types of failures that causes all three solenoids to fail to close can contribute to a shutdown failure in the dispenser.

For all the branches in the 100% dispenser leak fault tree under the “Accidents” and “Shutdown Failure” branches, the number was multiplied by 8760 refuelings per year, so that all values in the fault tree were converted to the same units before calculating risk.

3.2. Production, Compression, and Storage Area Risk

Based on the calculated leak frequencies of the components in the production, compression, and storage area, the compressor has the highest leak frequency, followed by the filter and valves, with the remainder of the components having relatively low leak frequencies. If risk mitigative actions are to be taken in relation to reducing leak frequencies of certain components, it would be most effective to target these components with higher leak frequencies.

The risk was calculated and visualized in both 1D and 2D space as shown below. Figure 3-4(a) shows the individual risk in annual frequency of fatality based only on distance away from the leak. This plot shows the most conservative scenario in which any leak is expected to be pointed directly at the person. This plot shows a reference metric of 2×10^{-5} fatalities per year, which is one measure of publicly accepted risk at gasoline refueling stations [16]. In general, risks tolerated or accepted for activities conducted by members of the public tend to be lower than those conducted by facility workers or operators. For example, the acceptable individual risk numbers used in NFPA 59A are lower for public areas and higher for land uses under the purview of a plant operator [17]. Other factors, such as operator training and possible PPE use compared to the general public conducting the same refueling task, may factor into the differences in accepted and actual risk to people at public and private refueling stations. Although this hydrogen bus fleet refueling station is not a public facility and could therefore potentially accept a higher risk, this metric is a helpful reference point. The plot in Figure 3-4(a) shows that the risk does not fall below 2×10^{-5} fatalities per year until the person is around 3 meters away from the leak. Figure 3-4(b) shows a 2D map of risk for a person at different locations around a leak, not necessarily only in front of it.

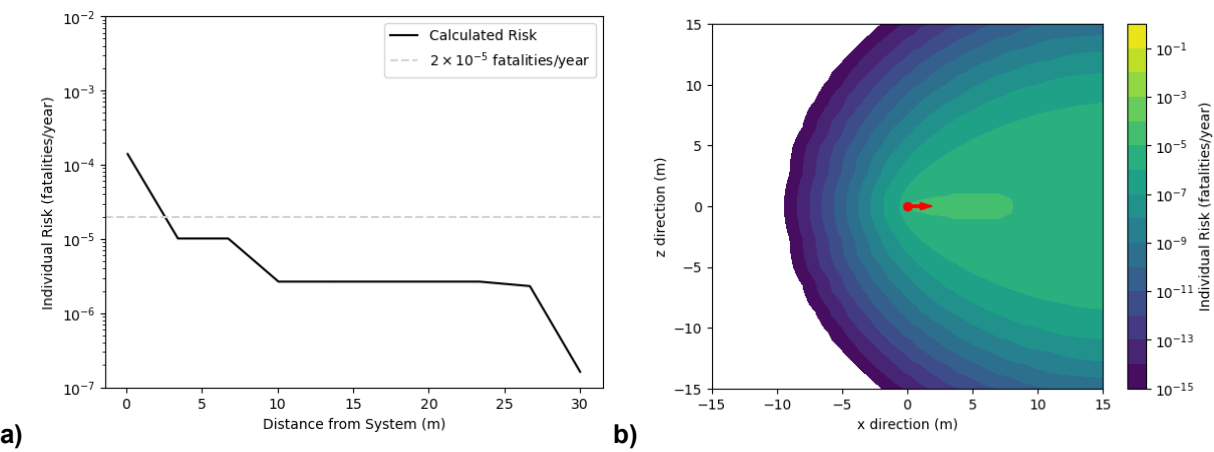


Figure 3-4. a) Risk based on distance from a leak, for a person assumed to be directly in front of the leak and b) risk based on location in relation to a leak for the production, compression, and storage area of the facility.

In Figure 3-4(b), the shape of the risk contour is similar to the shape of a heat flux contour from a jet fire. This shape likely came about for two reasons – first, immediate ignition is more likely to occur than delayed ignition, which is reflected in the default ignition probabilities in HyRAM+ [7],

[18]. Second, the consequence from explosive events is estimated to be generally low, partially because of the low default flame speed in HyRAM+. While a flame speed of Mach 0.35 is not always conservative, it may be more realistic than a higher flame speed because the system will be outdoors so there will probably be minimal congestion around which the flame will accelerate and cause a larger overpressure event [19].

Both plots in Figure 3-4 provide an indication of how far away a person must be, or where relationally a person must be, for their risk to drop below the reference risk metric. Isolation of the production, compression, and storage system using a structure such as an enclosing blast or fire wall could help contain potential risks within this area and reduce risk to people outside of the area.

Again, these risk results are not meant to reflect or be applied to specific hydrogen systems, because the QRA inputs were assumed based on generic and highly uncertain data.

3.3. Dispenser Area Risk

The fault trees in Section 3.1 show that, within the dispenser area, the chiller is the component type with the highest per-component annual leak frequency, followed by valves and then all other component types. It should be noted that the valves include the nozzle of the dispenser hose and the fueling receptacle on the fuel cell vehicle. Figure A-10 specifically also includes refueling-specific scenarios such as dispenser shutdown and accidents resulting in a 100% leak. The private nature of this refueling station, where all dispenser operators will be fully trained and required to follow specific protocols, may reduce the risk of accidents from the numbers shown in the fault tree. The failure probabilities in the fault tree were originally developed for public refueling facilities but are generic and highly uncertain. Similarly, the vehicles that will be refueled at this facility will also be part of a private fleet, which means that inspection and maintenance of the vehicles themselves can help drive down the risk of accidents involving both dispenser and vehicle.

Using a 24-vehicle fleet and an assumption of one fueling per vehicle per day for 365 days of the year, we calculated the annual frequency of failure for leaks from the dispenser to be 4.80×10^{-5} per year. Risk mitigation at the dispenser is important during design and operation of the facility. Some of the main components whose failures are closely tied to dispenser leaks are the breakaway coupling, the nozzle, and the manual and automatic solenoid valves on the dispenser. Developing a robust protocol for routine inspection and maintenance or replacement of these dispenser components is one possible way to reduce risk.

In terms of consequences, the components within the dispenser area have different heat flux and overpressure profiles for jet fire and explosion outcomes, based on whether they are before or after the chiller, since the fuel conditions affect the jet plume that forms from a leak. Lowering the temperature makes the plume more buoyant, while lowering the pressure makes it travel less far horizontally. Both effects could cause an individual leak from the chilled part of the system to pose a lower risk than the part of the system at ambient temperature. The contours of these consequences are included in Appendix B, and they indicate that there are slight but not substantial differences in the flame temperature, flame heat flux, and overpressure contours between the two subsystems.

The calculated risk for the dispenser area, by distance and location with respect to the system, is shown in Figure 3-5.

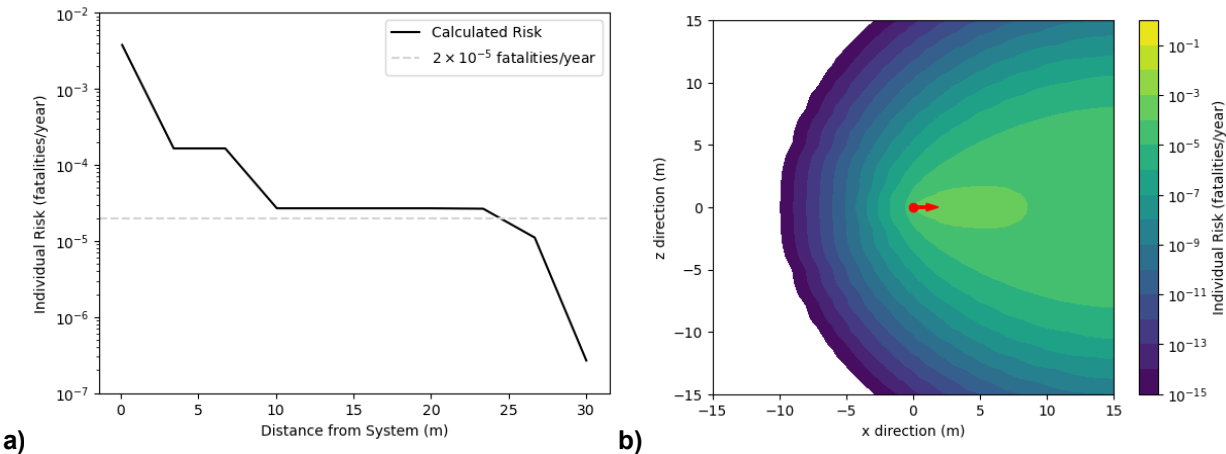


Figure 3-5. a) Risk based on distance from a leak, for a person assumed to be directly in front of the leak and b) risk based on location in relation to a leak for the dispenser area of the facility.

Compared to the production, storage, and compression area, the dispenser area seems to pose a greater risk for a person in the vicinity. The risk to a person near the dispenser system does not drop below the 2×10^{-5} fatalities per year until a distance of just before 25 meters away, compared to around 3 meters from the storage area. Similarly, comparing Figure 3-4(b) to Figure 3-5(b), it seems that, for many locations on the plot in relation to the system – particularly those in front of the leak – the annual risk of fatality is greater from the refueling system than the production, storage, and compression system. Again, this result is largely attributable to the leak frequencies of the components in each area. The dispenser area contains the chiller, which was modeled as a heat exchanger, which has the highest leak frequency of all the components included in the QRA.

3.4. Risk Reduction Through Prevention and Mitigation

Both hazard prevention and risk mitigation actions can be taken to improve safety of an FCEB refueling station such as the one discussed in this report. Table 3-1 shows how these actions can be prioritized to reduce overall risk. Stakeholders designing a hydrogen facility such as the production and dispensing system discussed in this report can prioritize hydrogen leak prevention; however, if leaks do occur, the second-priority category of mitigation actions may focus on preventing ignition of the hydrogen and the possible formation of jet fires or explosions. The last layer of protective actions is relevant if a leak and ignition event occur – in this case, people must be protected from areas where the ignition event is occurring, whether through isolation and distance or a physical barrier.

Table 3-1. Priorities for Consequence and Risk Mitigation Actions

Priority	Category	Description	Causes	Actions
1	Leak prevention	Preventing releases of hydrogen from the system	<ul style="list-style-type: none"> General wear of system components over time Cracking/damage from hydrogen embrittlement Unintended mechanical impacts Extreme weather events or natural disasters (e.g., seismic events, high wind, hail) 	<ul style="list-style-type: none"> Protocols requiring regular inspection, maintenance, repair, and replacement of components (with priority for components with highest leak frequencies) Implementation of barriers/bollards to prevent unintended activities or accidents (e.g., driving) in areas with hydrogen equipment Posted signage (e.g., allowed locations for vehicles, speed limits) Equipment hardening against major threats (e.g., natural disasters common to the region in which the facility is located) and for especially vulnerable components Automatic detection systems and emergency shutdown and isolation systems for location-specific natural disaster conditions
2	Ignition prevention	Preventing ignition events (jet fires and explosions) once a hydrogen leak has occurred	<ul style="list-style-type: none"> High probabilities of ignition due to high leak flow rates Facility design with confined and/or congested spaces that allow for leaking hydrogen to accumulate and accelerate, potentially causing faster flame fronts and higher overpressure and impulse explosions Presence of ignition sources near hydrogen equipment 	<ul style="list-style-type: none"> Installation of sensors and automatic shutdown/shutoff valves near components with the highest leak frequencies to detect and shut down leaks early on Lowering of ignition probabilities via lowering of leak flow rate, if allowed by other system design parameters (e.g., lowering system pressure, using smaller-diameter components) Minimize confined and congested spaces (construct the system in a way that allows for leaking hydrogen to freely disperse) Signage and protocols preventing introduction of

Priority	Category	Description	Causes	Actions
				ignition sources into areas where hydrogen may be present (e.g., no smoking in facility, no hot work for repairs until hydrogen has been flushed from system)
3	Risk mitigation	Reducing harm to people and infrastructure once an ignition event has occurred	<ul style="list-style-type: none"> Presence of people or fragile infrastructure in ignition event impact zones (i.e., jet fires or explosions) 	<ul style="list-style-type: none"> Installation of fire or explosion barriers between the system and areas where people are working Implementation of detection and alarm systems to alert facility occupants of the presence of a hydrogen leak and/or fire Regular training for personnel (e.g., system operators) incorporating emergency protocols like site evacuation and personnel accounting Implementation of remote and automatic system controls to reduce amount of time that operators must be in the vicinity of the facility

As briefly mentioned, risk mitigations and design decisions are also influenced by factors such as cost, space, and feasibility. This QRA can be helpful for understanding relative contributions of different threats to overall system risk so risk mitigation actions can be prioritized and balanced with these other considerations. It must also be balanced with these aspects. For example, while the dispensing system may pose a relatively higher risk to people close to the system, the operations are likely to be unautomated and dependent on people (including those driving the buses and those conducting the refueling operations). Thus, possibly, preventive actions such as training and reduction of system leaks through regular inspection may be more effective overall than mitigations such as fire or blast wall implementation, which could hinder normal operations.

4. CONCLUSION

PDX is exploring the use of hydrogen FCEBs. We conducted a QRA for the everyday operations of a generic hydrogen FCEB facility; some insights, as well as the methodology, can be applied to other case studies, locations, and situations.

We split the QRA into two parts – one included the area where the hydrogen is produced, stored, and compressed, and the other included the dispensing area where the buses are refueled with hydrogen. We focused on risk to people in the vicinity, in terms of annual frequency of fatality, which we calculated using component leak frequencies, ignition probabilities, probit models for jet fire and explosion outcomes, and consequence severities (i.e., heat flux intensity and overpressure for jet fires and explosions, respectively). We created custom fault trees to calculate component leak frequencies and event sequence diagrams to calculate ignition probabilities. We used HyRAM+ to calculate the overall risk using these inputs.

For the system setup defined in this report, the dispensing area poses a higher risk to people in the facility, largely because the chiller (modeled as a heat exchanger) has a high leak frequency. The risk from this dispensing area drops below a comparable level of risk from a public gasoline refueling station of 2×10^{-5} fatalities per year once the person is almost 25 meters away from the leak, compared to the level of risk dropping below this accepted level around 3 meters away from the production, storage, and compression area.

There are several risk mitigations that could improve safety in the everyday operations of an FCEB facility, with major mitigations including reduction of component leak frequencies through inspection and maintenance of components with highest leak frequencies, regular training of personnel in facility operations, and strategic placement of fire and blast barrier walls to protect people and prevent major cascading failures in the system.

The risk results in this study are not meant to be absolute numbers that can be used to make design and operational decisions for either individual hydrogen systems or to generate overall regulatory guidance. However, this study can be valuable to stakeholders such as decision-makers for FCEB operations (whether at airports, or for general public transit or other applications), system designers, and regulators in the hydrogen, transportation, and/or vehicle areas. The QRA approach can inform safe design and general regulation of these FCEB-serving facilities, especially since there is not currently a largely established regulatory landscape in this space.

REFERENCES

- [1] "Portland International Airport (PDX) Backgrounder," Port of Portland, 2018.
- [2] O. Peckham, "PDX and PNNL Explore Hydrogen Fueling for Hazard Resilience," Fuel Cell Works, 2025.
- [3] "Portland Resilient Runway Benefit-Cost Analysis: An Overview," The National Institute of Building Sciences, 2021.
- [4] B. M. Wofford, M. S. Louie and M. Milletic, "Safety Hazards of Batteries and Hydrogen Storage Systems in Proximity," Sandia National Laboratories, Publication in Progress.
- [5] New Flyer, "xcelsior Charge FC Our next generation, fuel cell electric, zero emission transit bus," [Online]. Available: <https://www.newflyer.com/site-content/uploads/2024/07/Xcelsior-CHARGE-FC-Brochure.pdf>. [Accessed 4 November 2024].
- [6] S. Wiryadinata and E. S. Hecht, "Reference Station Design for Heavy-Duty Vehicles," Sandia National Laboratories, SAND2023-13773, Albuquerque, NM, 2023.
- [7] B. D. Ehrhart, C. Sims, E. S. Hecht, B. B. Schroeder, B. R. Liu, K. M. Groth, J. T. Reynolds and G. W. Walkup, "HyRAM+ (Hydrogen Plus Other Alternative Fuels Risk Assessment Models), Version 5.1.1," Sandia National Laboratories, SAND2023-14224, Albuquerque, NM, 2024.
- [8] R. Caponi, A. M. Ferrario, E. Bocci, S. Bodker and L. del Zotto, "Single-tank storage versus multi-tank cascade system in hydrogen refueling stations for fuel cell buses," vol. 47, no. 64, 2022.
- [9] D. M. Brooks, M. S. Louie and B. D. Ehrhart, "Updated Filter Leak Frequencies for Use in Risk Assessments," Sandia National Laboratories, SAND2024-06491, Albuquerque, NM, 2024.
- [10] Hyfindr, *Tech Talk - Hydrogen Refueling Station - Hydrogen Fuel Cell Technology Explained - Hyfindr Mariacher*, 2023.
- [11] Hyfindr, *Tech Talk - Cascade Management in Hydrogen Refueling - Hydrogen Technology Explained - Hyfindr Schoni*, YouTube, 2023.
- [12] N. Eisenberg, C. Lynch and R. Breeding, "Vulnerability model: A simulation system for assessing damage resulting from marine spills," U.S. Coast Guard, Technical Report SA/A-015 245, 1975.
- [13] "Methods for the determination of possible damage," The Netherlands Organization of Applied Scientific Research (TNO), Technical Report CPR 16E, 1992.
- [14] J. LaChance, A. Tchouvelev and A. Engebo, "Development of uniform harm criteria for use in quantitative risk analysis of the hydrogen infrastructure," *International Journal of Hydrogen Energy*, vol. 36, no. 3, pp. 2381-2388, 2011.
- [15] J. LaChance, W. Houf, B. Middleton and L. Fluer, "Analyses to Support Development of Risk-Informed Separation Distances for Hydrogen Codes and Standards," Sandia National Laboratories, SAND2008-0874, Albuquerque, NM and Livermore, CA, 2009.
- [16] D. Diamantidis, *Background Documents on Risk Assessment in Engineering: Risk Acceptance Criteria*, Joint Committee of Structural Safety, 2008.

- [17] B. D. Erhart, D. Brooks, A. B. Muna and C. LaFleur, "Evaluation of Risk Acceptance Criteria for Transporting Hazardous Materials," U.S. Department of Transportation, DOT/FRA/ORD-20/06, 2020.
- [18] A. V. Tchouvelev, "Knowledge gaps in hydrogen safety: A white paper," International Energy Agency Hydrogen Implementing Agreement Task 19, January 2008.
- [19] S. Jallais, E. Vyazmina, D. Miller and J. K. Thomas, "Hydrogen jet vapor cloud explosion: A model for predicting blast size and application to risk assessment," *Process Safety Progress*, vol. 37, no. 3, pp. 397-410, 2018.
- [20] A. Veeramany, B. M. Marten, B. Mamnani, M. S. Louie, M. Miletic and B. D. Ehrhart, "Hydrogen Transportation and Distributed Energy Systems Seismic Risk Assessment for Cascadia Subduction Zone Airport Facilities (CRADA 555)," Pacific Northwest National Laboratory, Publication in Progress.

Appendix A. Fault and Event Trees Used for QRA

A.1. Fault Trees

Generic fault trees for the components in the overall facility are provided in this Appendix. As discussed in Section 2 of this report, the QRA was split into two sections, and for simplicity, separate fault trees were developed for each section. For both sections (the production/compression/storage section and the dispensing section) of the facility, a fault tree was developed for each leak size.

A.1.1. *Production, Storage, and Compression Area*

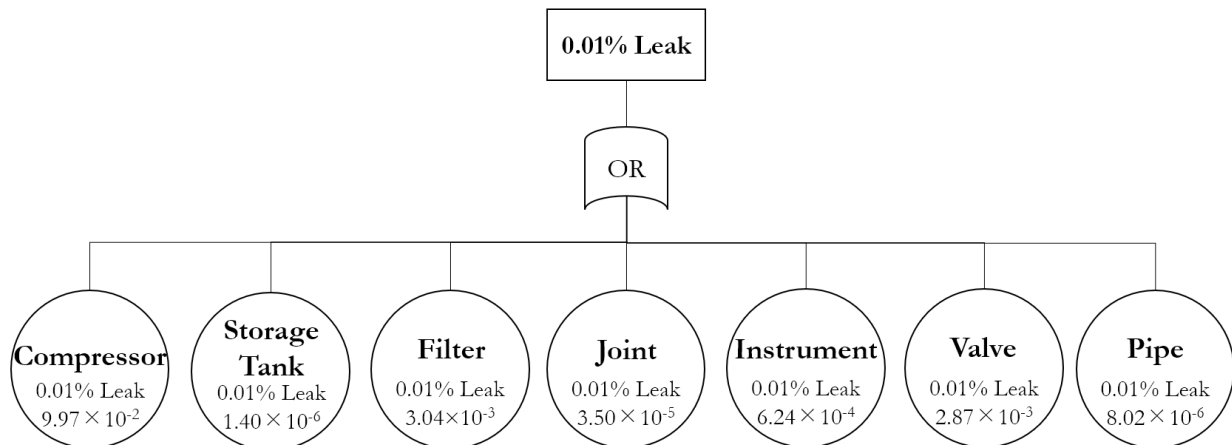


Figure A-1. Generic fault tree for 0.01% leak from the storage and compression area. Provided numbers are per-component median annual leak frequencies for a single instance of each included component.

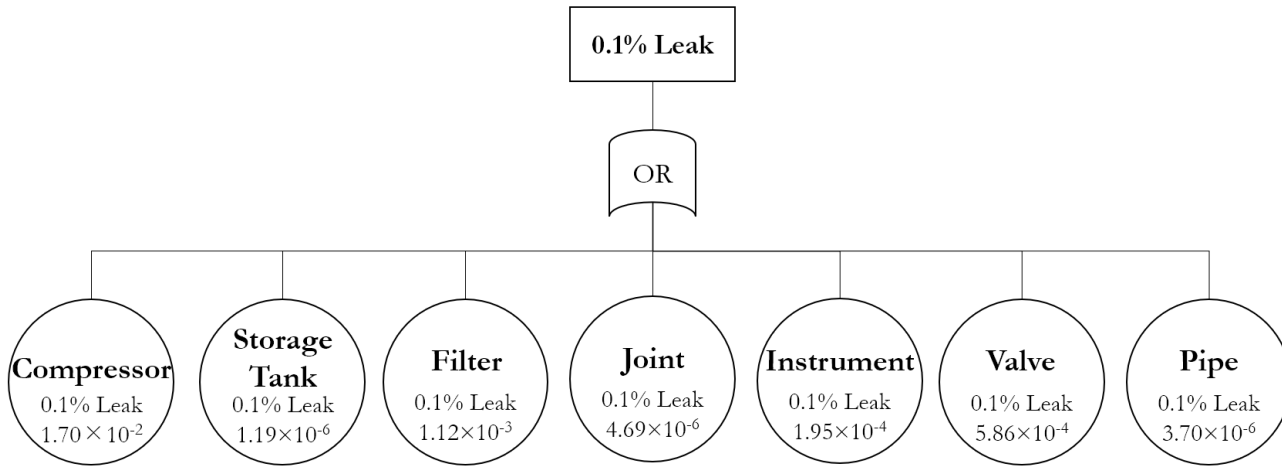


Figure A-2. Generic fault tree for 0.1% leak from the storage and compression area. Provided numbers are per-component median annual leak frequencies for a single instance of each included component.

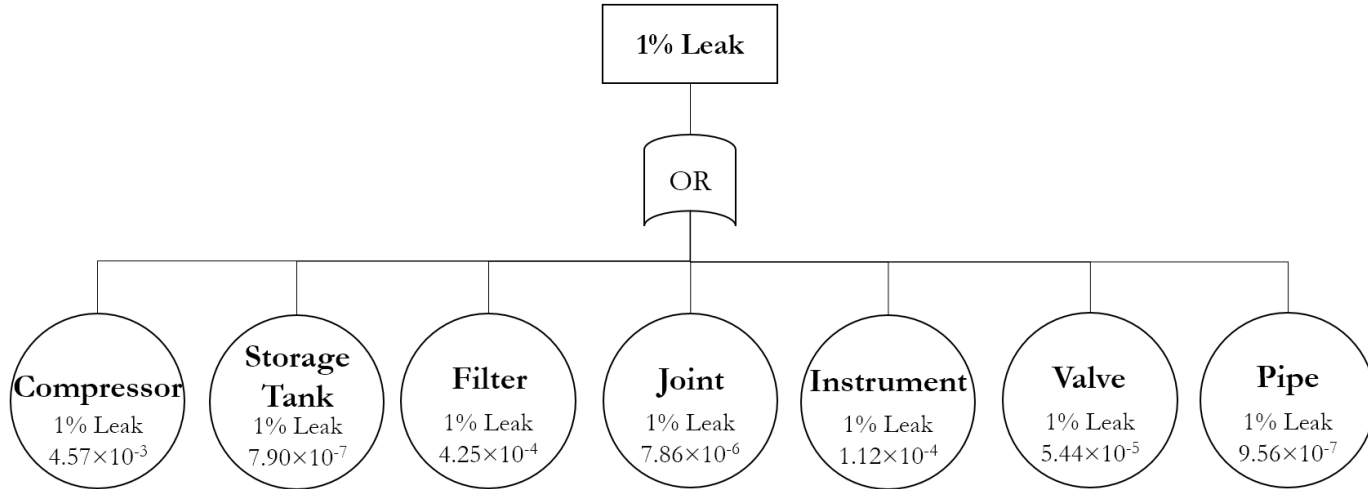


Figure A-3. Generic fault tree for 1% leak from the storage and compression area. Provided numbers are per-component median annual leak frequencies for a single instance of each included component.

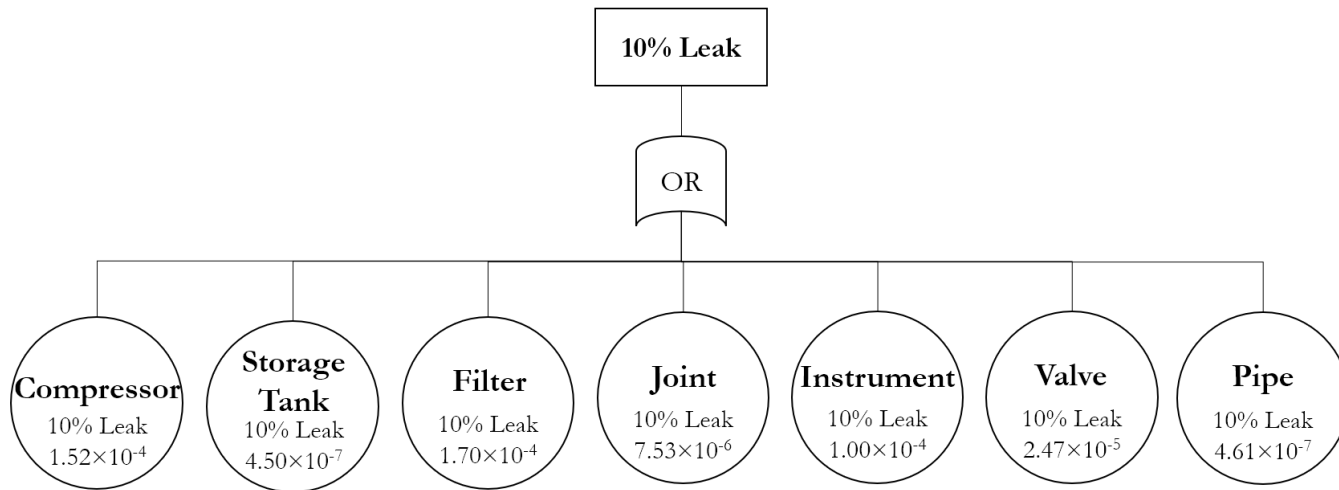


Figure A-4. Generic fault tree for 10% leak from the storage and compression area. Provided numbers are per-component median annual leak frequencies for a single instance of each included component.

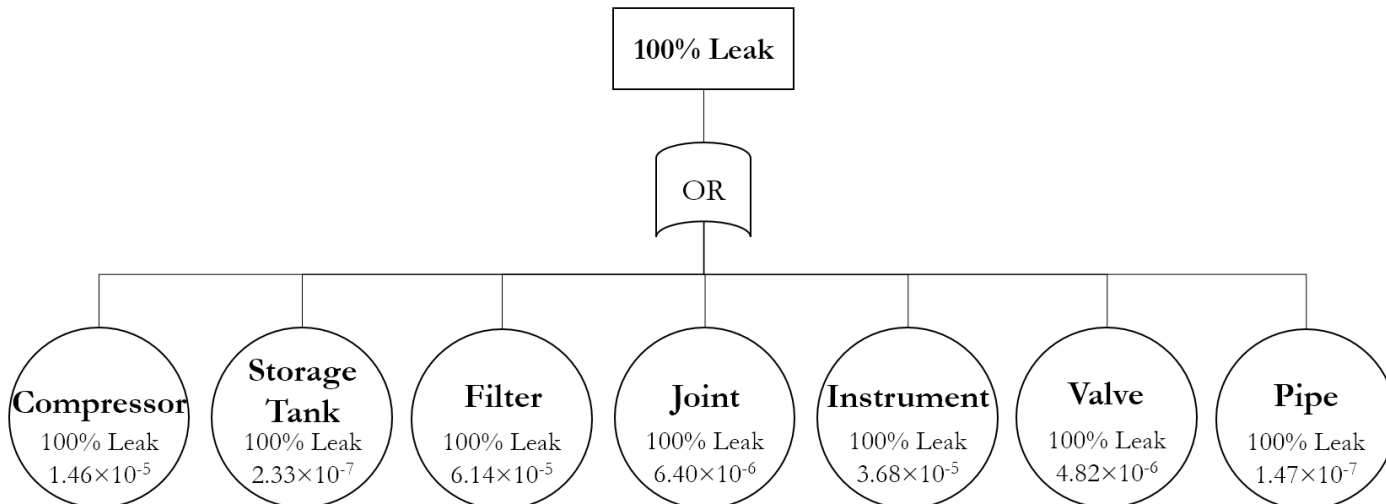


Figure A-5. Generic fault tree for 100% leak from the storage and compression area. Provided numbers are per-component median annual leak frequencies for a single instance of each included component.

A.1.2. Dispensing Area

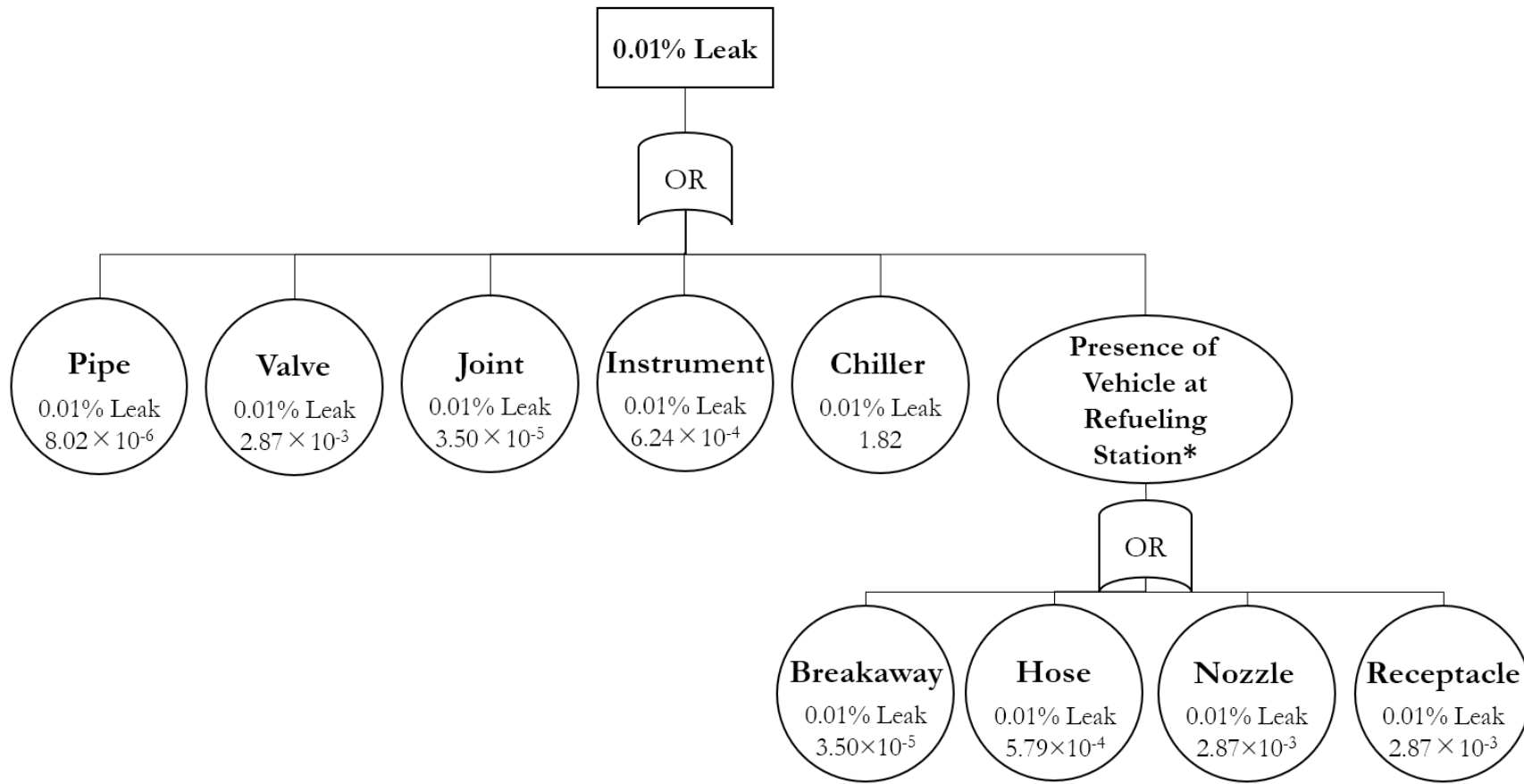


Figure A-6. Generic fault tree for 0.01% leak from the dispensing area. Provided numbers are per-component median annual leak frequencies for a single instance of each included component. * indicates that the frequencies below were multiplied by the assumed total refueling time per year.

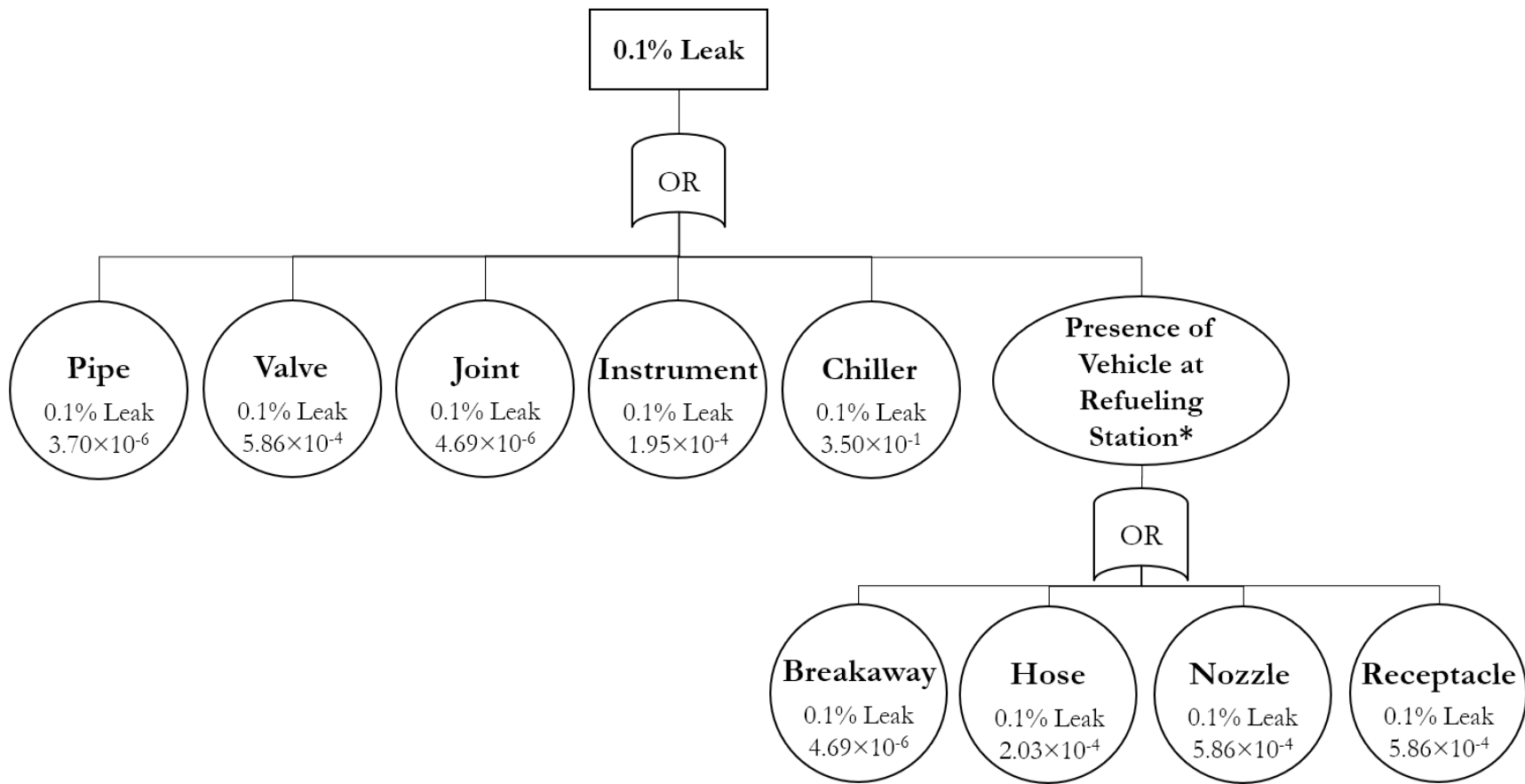


Figure A-7. Generic fault tree for 0.1% leak from the dispensing area. Provided numbers are per-component median annual leak frequencies for a single instance of each included component. * indicates that the frequencies below were multiplied by the assumed total refueling time per year.

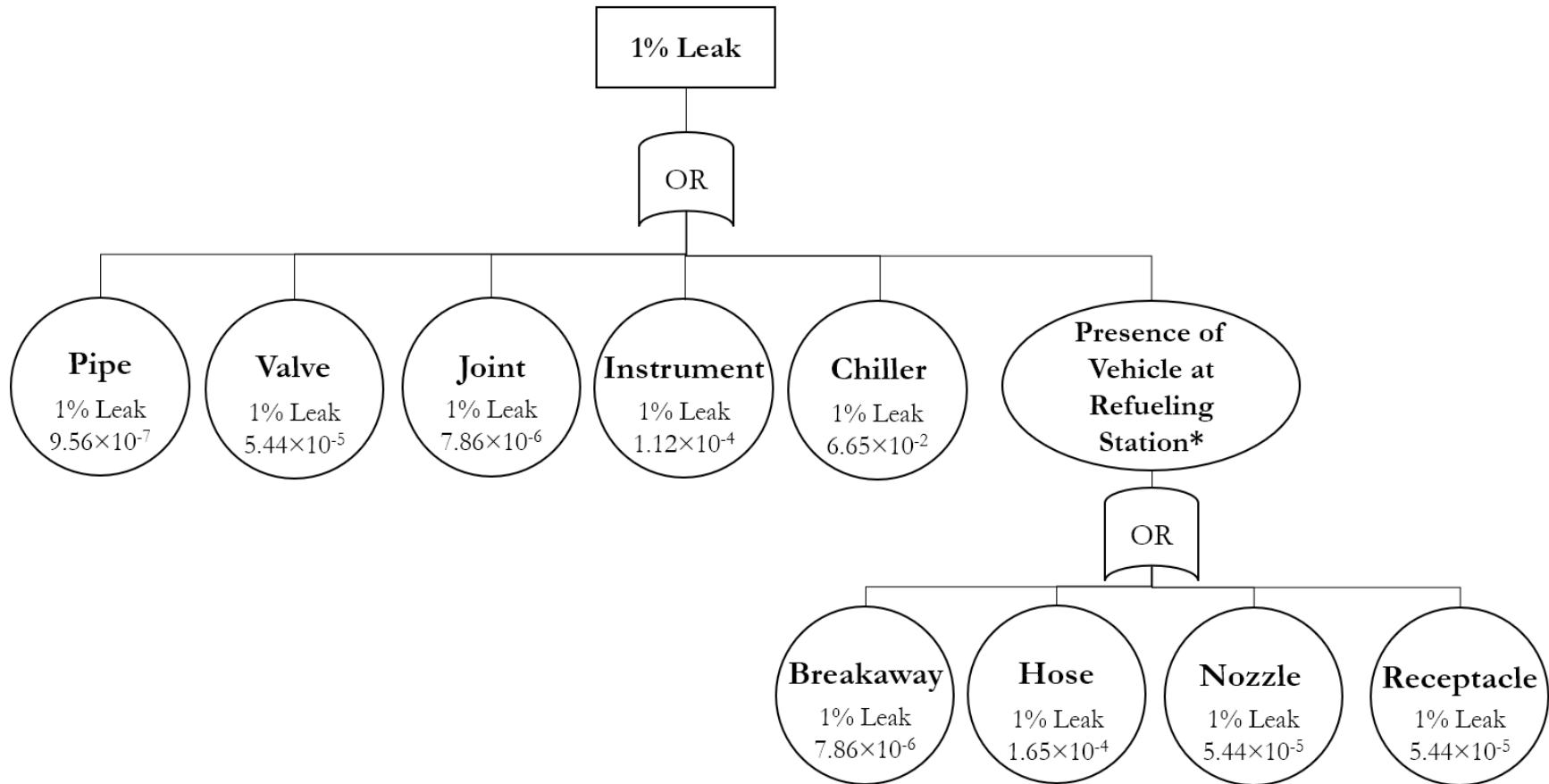


Figure A-8. Generic fault tree for 1% leak from the dispensing area. Provided numbers are per-component median annual leak frequencies for a single instance of each included component. * indicates that the frequencies below were multiplied by the assumed total refueling time per year.

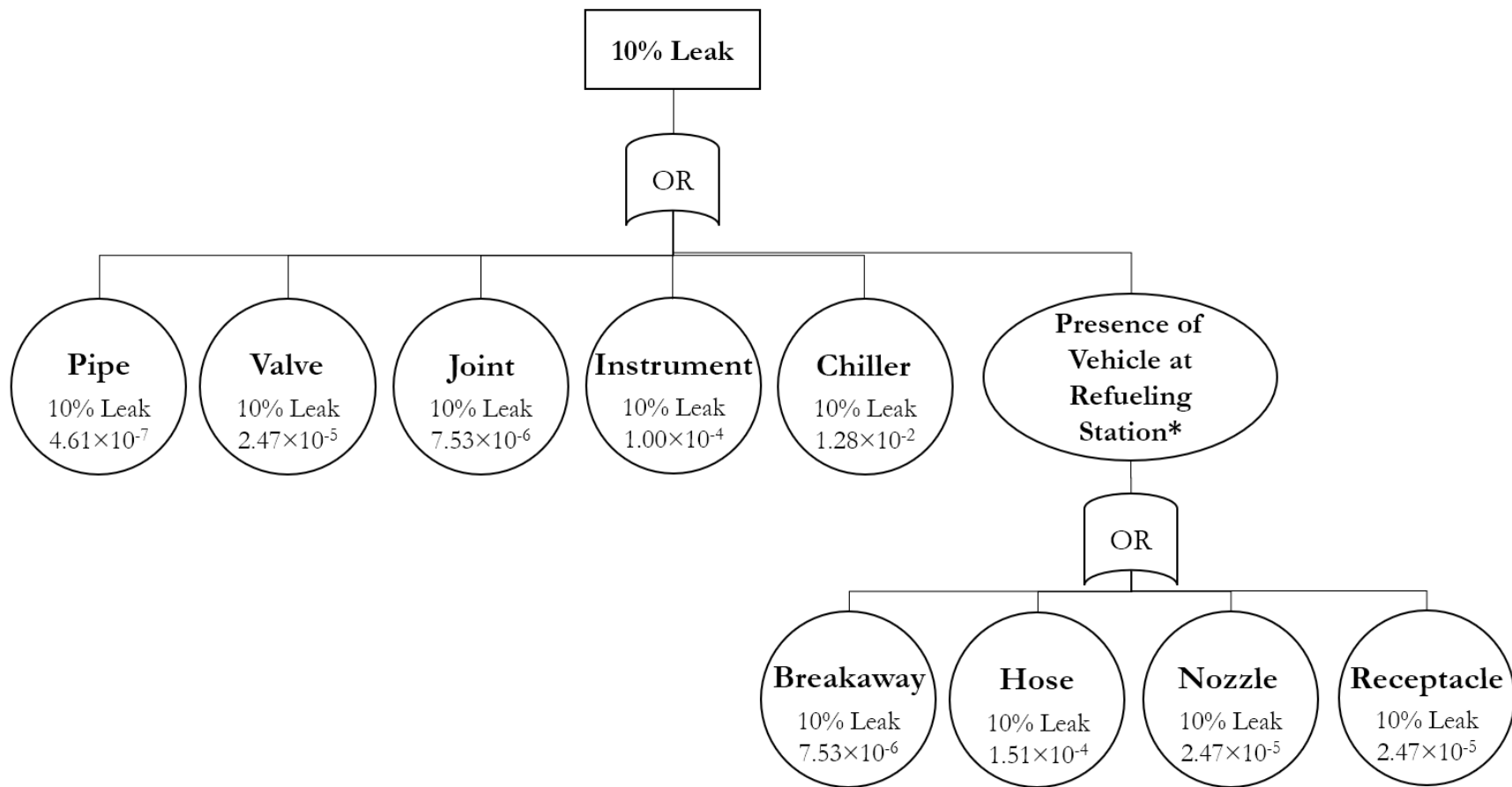


Figure A-9. Generic fault tree for 10% leak from the dispensing area. Provided numbers are per-component median annual leak frequencies for a single instance of each included component. * indicates that the frequencies below were multiplied by the assumed total refueling time per year.

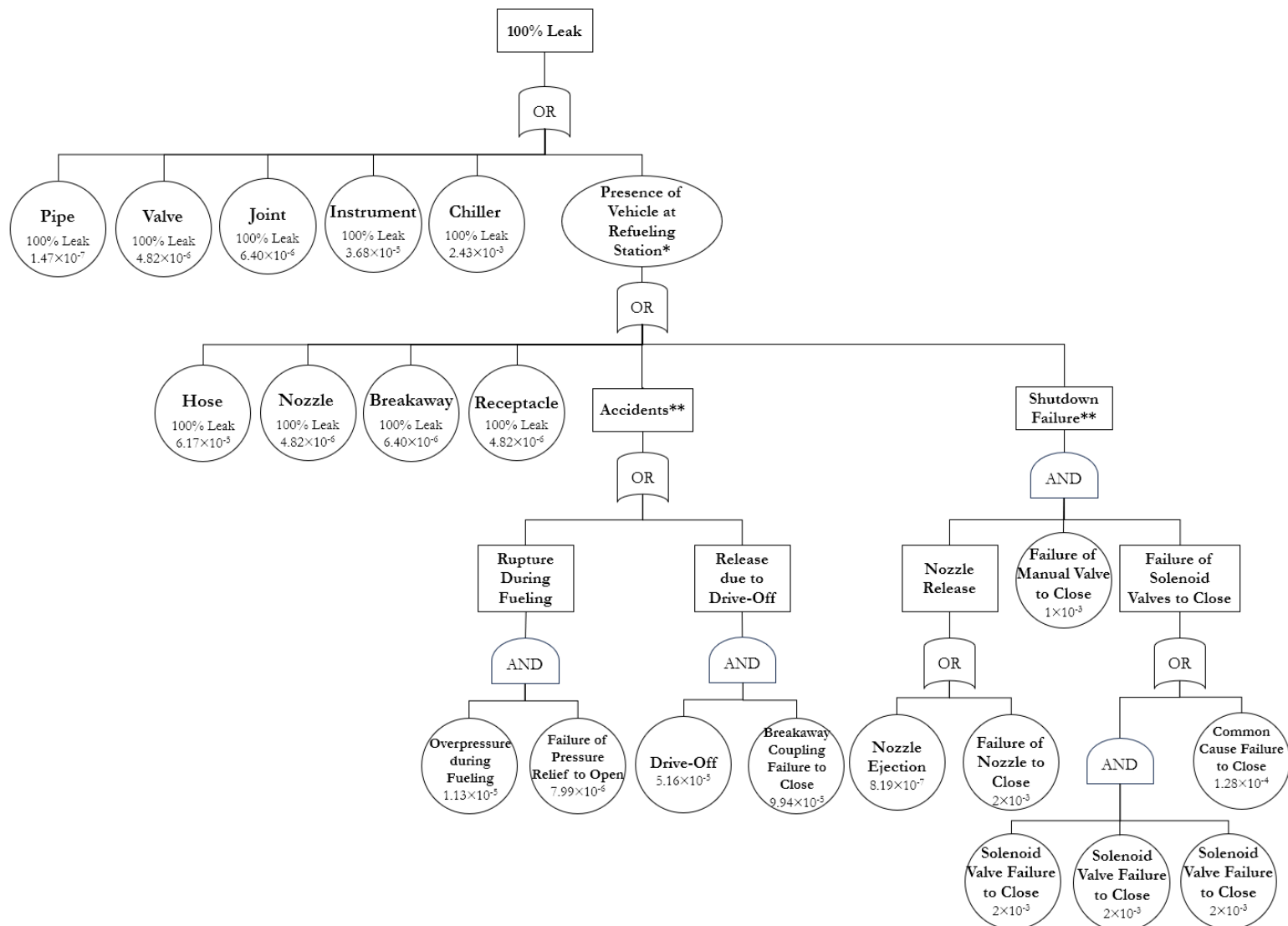


Figure A-10. Generic fault tree for 100% leak from the dispensing area. Provided numbers are per-component median annual leak frequencies for a single instance of each included component except for **, which are leak probabilities per refueling. * indicates that the frequencies below were multiplied by the assumed total refueling time per year.

A.1.3. Fault Tree Data

This section contains the tabulated fault tree data. Note that, though the vehicle components are categorized in their own section, they would be present near the dispenser during refueling and are therefore included in the dispenser QRA [7].

Table A-1. Component Annual Median Operational Leak Frequencies by Leak Size for Components in Gaseous Hydrogen Systems.

Component	HyRAM+ Component Name	Median Leak Frequency (per year)				
		0.01%	0.1%	1%	10%	100%
PRODUCTION, COMPRESSION, AND STORAGE AREA						
Electrolyzer	No equivalent	Insufficient data available				
Compressor	Compressor	9.97×10^{-2}	1.70×10^{-2}	4.57×10^{-3}	1.52×10^{-4}	1.46×10^{-5}
Storage Tank	Vessel	1.40×10^{-6}	1.19×10^{-6}	7.90×10^{-7}	4.50×10^{-7}	2.33×10^{-7}
Filter	Filter	3.04×10^{-3}	1.12×10^{-3}	4.25×10^{-4}	1.70×10^{-4}	6.14×10^{-5}
Joint	Joint	3.50×10^{-5}	4.69×10^{-6}	7.86×10^{-6}	7.53×10^{-6}	6.40×10^{-6}
Instrument	Instrument	6.24×10^{-4}	1.95×10^{-4}	1.12×10^{-4}	1.00×10^{-4}	3.68×10^{-5}
Valve	Valve	2.87×10^{-3}	5.86×10^{-4}	5.44×10^{-5}	2.47×10^{-5}	4.82×10^{-6}
Pipe	Pipe	8.02×10^{-6}	3.70×10^{-6}	9.56×10^{-7}	4.61×10^{-7}	1.47×10^{-7}
DISPENSER AREA						
Pipe	Pipe	8.02×10^{-6}	3.70×10^{-6}	9.56×10^{-7}	4.61×10^{-7}	1.47×10^{-7}
Valve	Valve	2.87×10^{-3}	5.86×10^{-4}	5.44×10^{-5}	2.47×10^{-5}	4.82×10^{-6}
Joint	Joint	3.50×10^{-5}	4.69×10^{-6}	7.86×10^{-6}	7.53×10^{-6}	6.40×10^{-6}
Instrument	Instrument	6.24×10^{-4}	1.95×10^{-4}	1.12×10^{-4}	1.00×10^{-4}	3.68×10^{-5}
Chiller	Heat Exchanger	1.82	3.50×10^{-1}	6.65×10^{-2}	1.28×10^{-2}	2.43×10^{-3}
Breakaway	Joint	3.50×10^{-5}	4.69×10^{-6}	7.86×10^{-6}	7.53×10^{-6}	6.40×10^{-6}
Hose	Hose	5.79×10^{-4}	2.03×10^{-4}	1.65×10^{-4}	1.51×10^{-4}	6.17×10^{-5}
Nozzle	Valve	2.87×10^{-3}	5.86×10^{-4}	5.44×10^{-5}	2.47×10^{-5}	4.82×10^{-6}
FUEL CELL VEHICLE						
Receptacle (on vehicle)	Valve	2.87×10^{-3}	5.86×10^{-4}	5.44×10^{-5}	2.47×10^{-5}	4.82×10^{-6}
Fuel Cell	No equivalent	Insufficient data available				
Fueling Receptacle	No equivalent	Insufficient data available				
Onboard Storage Tank	No equivalent	Insufficient data available				

Table A-2. Dispenser-Specific Median Leak Probabilities per Refueling.

COMPONENT FAILURES		
Component	Failure Mode	Median Leak Probability During Refueling
Nozzle	Pop-off	8.19×10^{-7}
	Failure to close	2×10^{-3}
Breakaway coupling	Failure to close	9.94×10^{-5}
Pressure relief valve	Failure to open	7.99×10^{-6}
Manual valve	Failure to close (human error)	1×10^{-3}
Solenoid valve	Failure to close	2×10^{-3}
	Common cause failure	1.28×10^{-4}
ACCIDENT FAILURES		
Accident Type	Median Leak Probability During Refueling	
Drive-off	5.16×10^{-5}	
Overpressure during fueling	1.13×10^{-5}	

A.2. Event Sequence Diagram

The event sequence diagrams shown in Figure A-11 and Figure A-12 show how the annual frequency of each ignition event was calculated for each leak size, based on the annual leak frequency, the probability of detection and isolation of the leak without the occurrence of an ignition event, and immediate, delayed, or no ignition, based on the ignition probabilities and the flow rate of the leak [7].

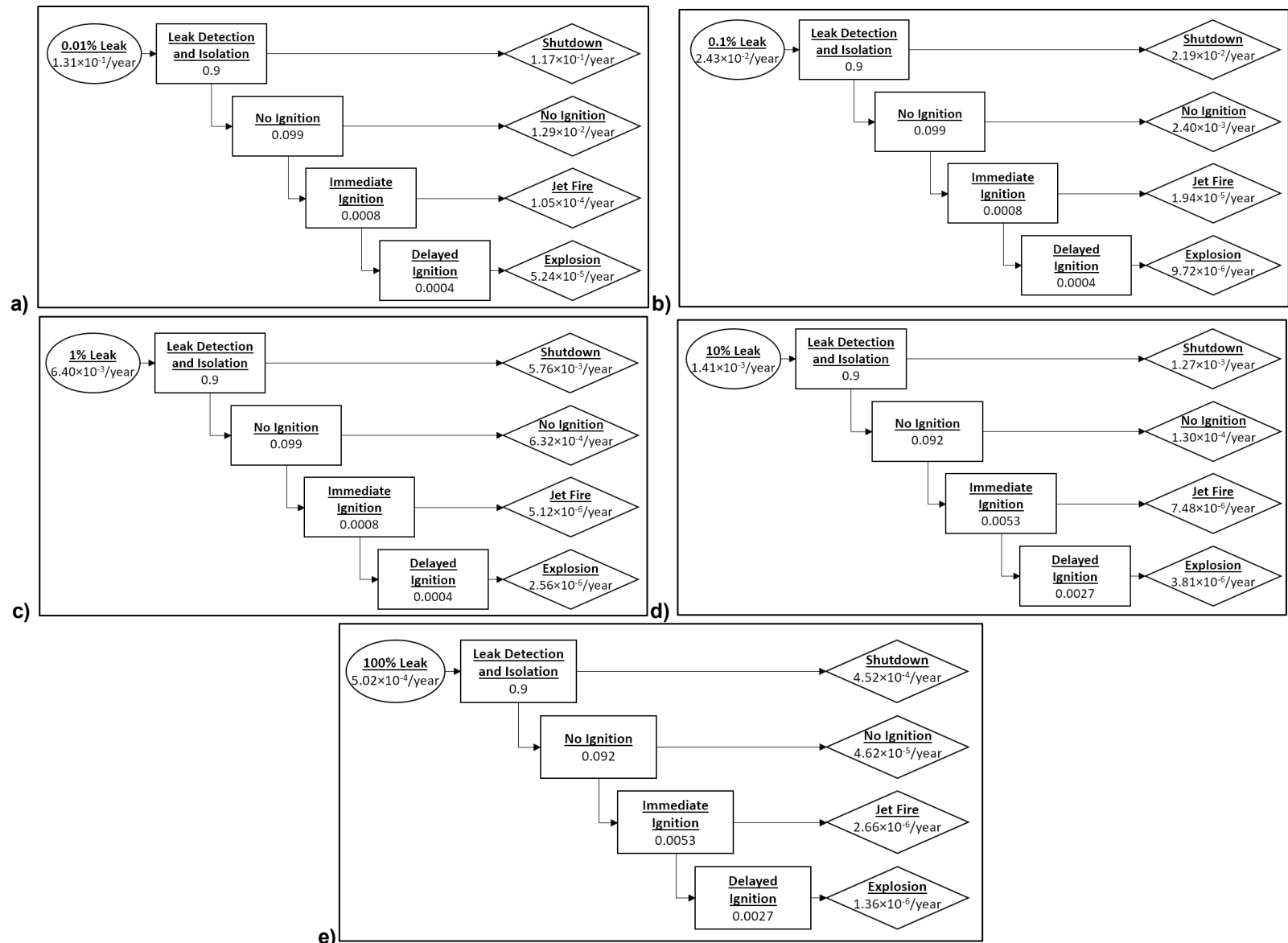


Figure A-11. Event sequence diagram with probabilities (rectangles) and annual frequencies (non-rectangles) for a) 0.01%, b) 0.1%, c) 1%, d) 10%, and e) 100% leak for the production, compression, and storage area.

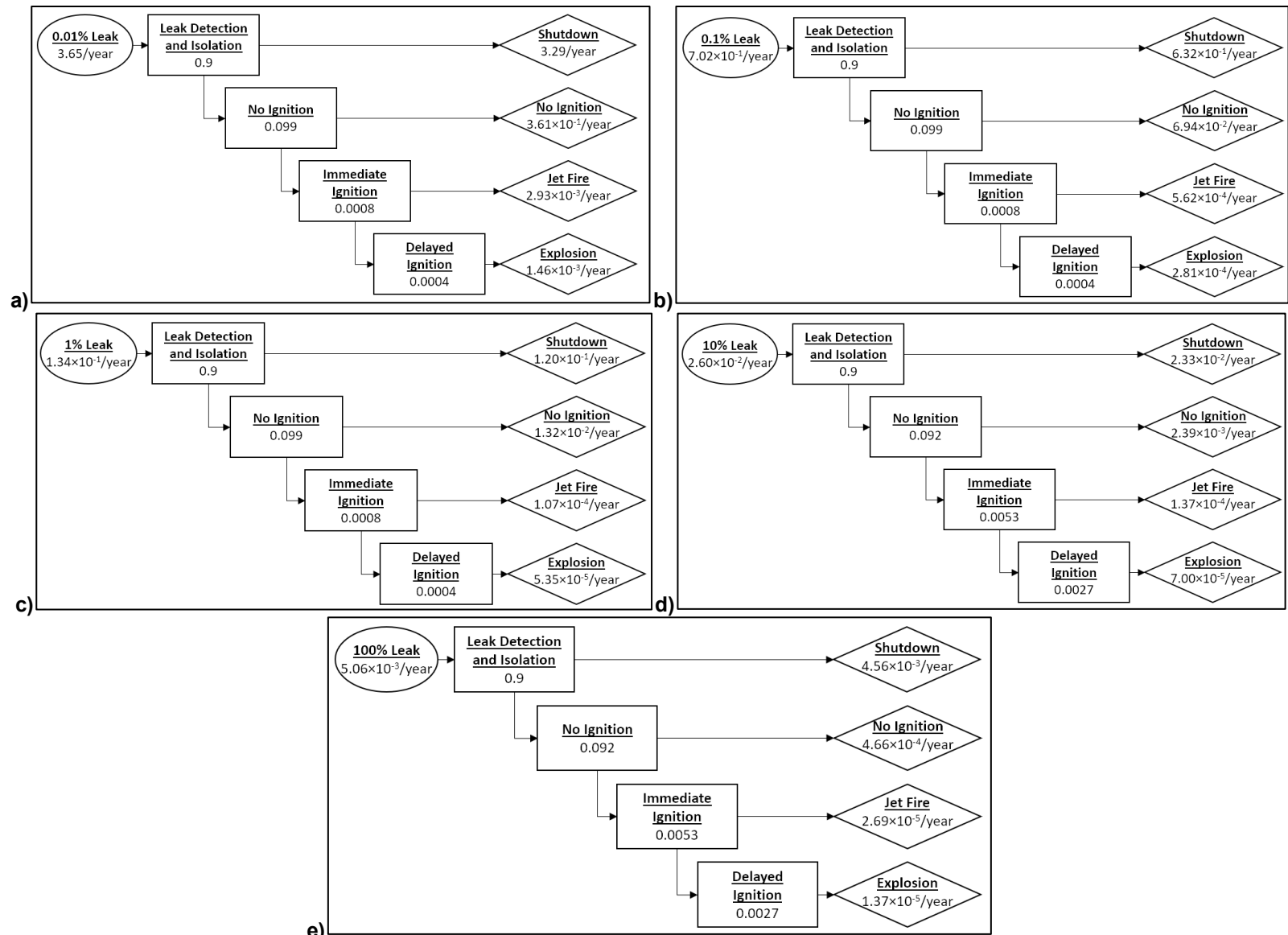


Figure A-12. Event sequence diagram with probabilities (rectangles) and annual frequencies (non-rectangles) for a) 0.01%, b) 0.1%, c) 1%, d) 10%, and e) 100% leak from dispenser area.

APPENDIX B. HAZARD CONTOURS

This Appendix shows contours for the consequences of each leak size, for both areas of the overall facility, for immediate ignition (resulting in a jet fire) and delayed ignition (resulting in an explosion).

B.1. Jet Fire Consequences

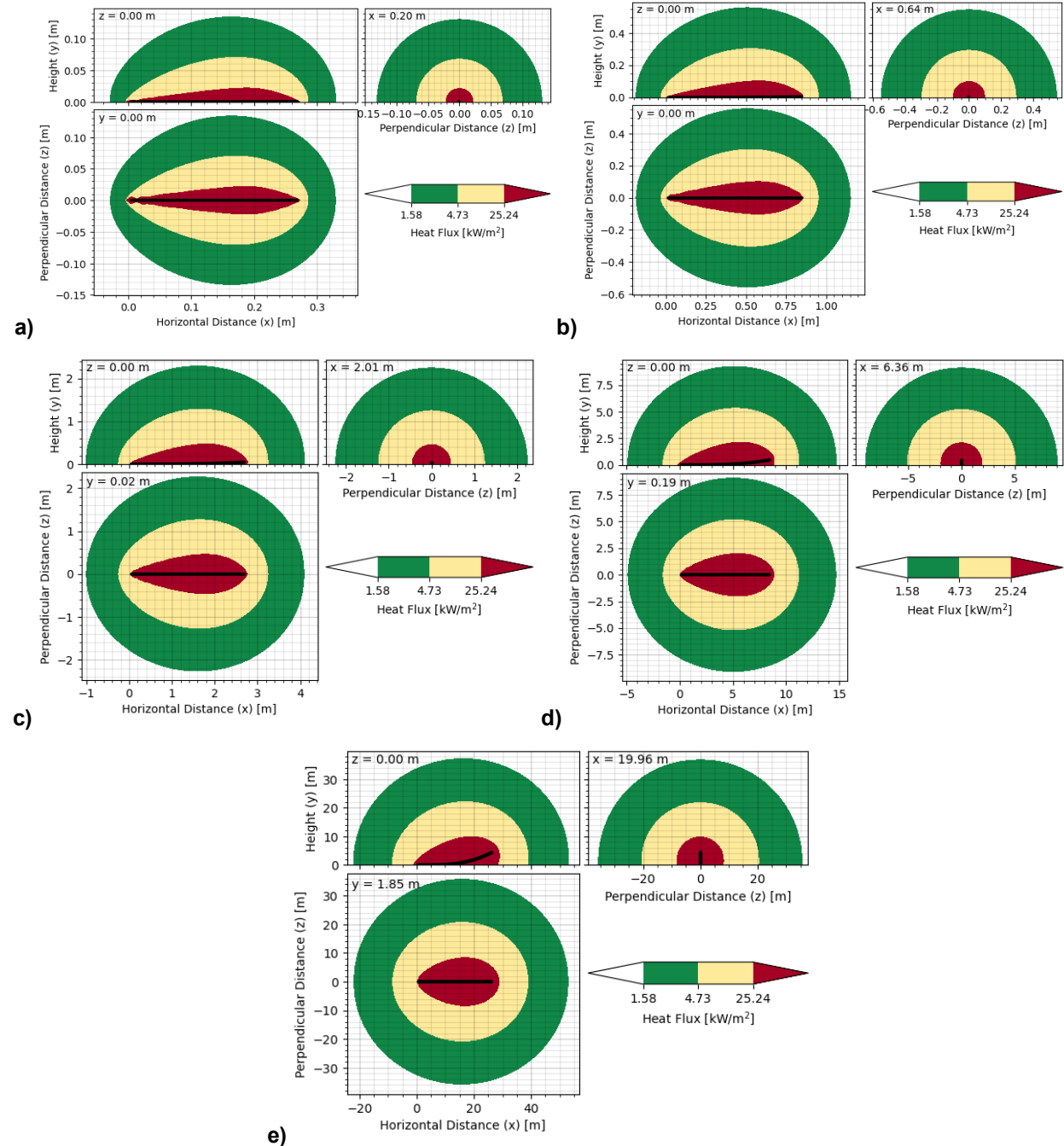


Figure B-13. Heat flux contours from a jet fire from a) 0.01%, b) 0.1%, c) 1%, d) 10%, and e) 100% leak directed in the +x direction, for components before the chiller carrying hydrogen at 20°C (68°F) and 900 bar (13,053 psi). x values are in the direction of the leak, z values are perpendicular to the leak, and y values correspond to height.

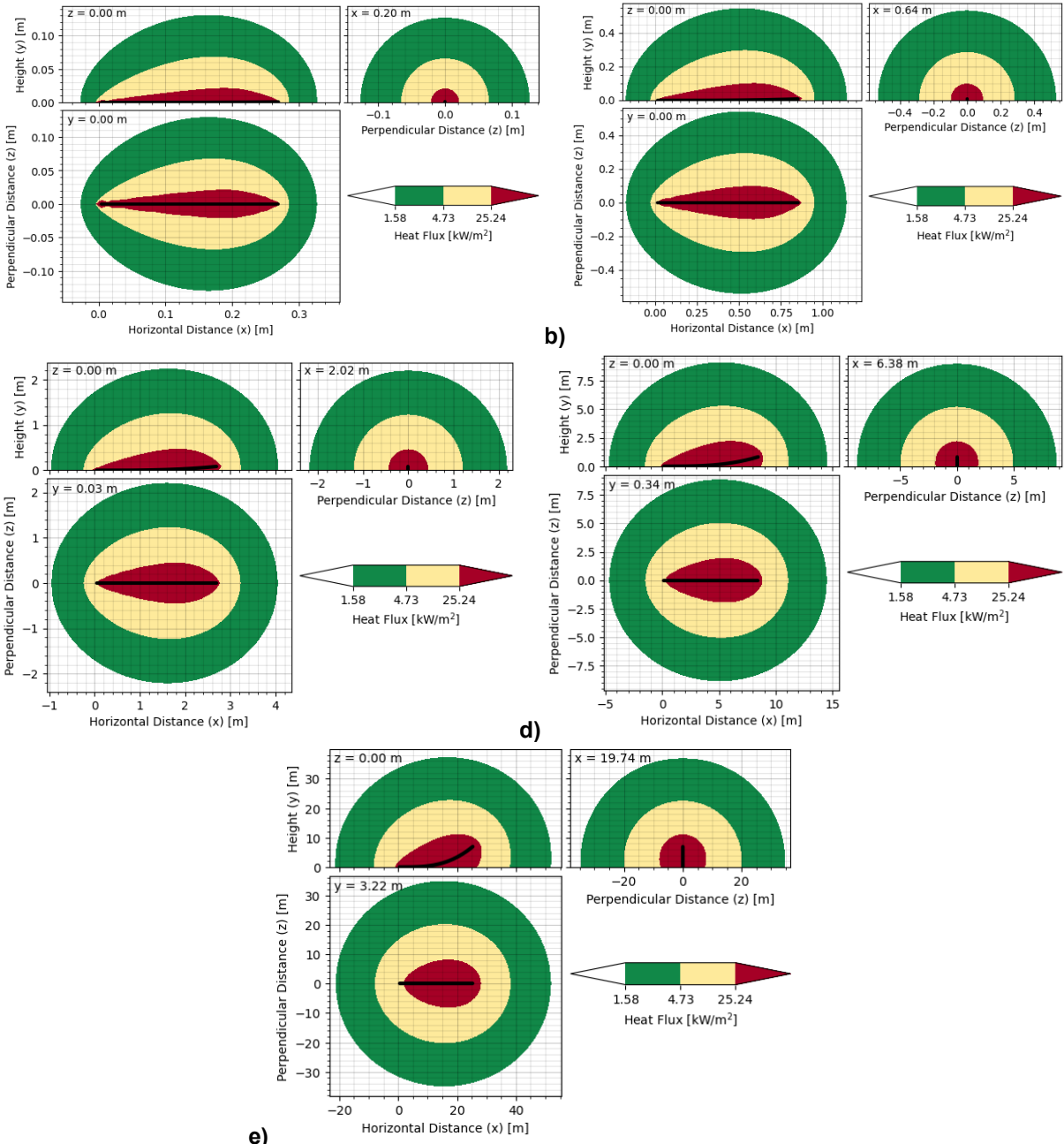


Figure B-14. Heat flux contours from a jet fire from a) 0.01%, b) 0.1%, c) 1%, d) 10%, and e) 100% leak directed in the +x direction, for components after the chiller carrying hydrogen at -40°C (-40°F) and 700 bar (10,153 psi). x values are in the direction of the leak, z values are perpendicular to the leak, and y values correspond to height.

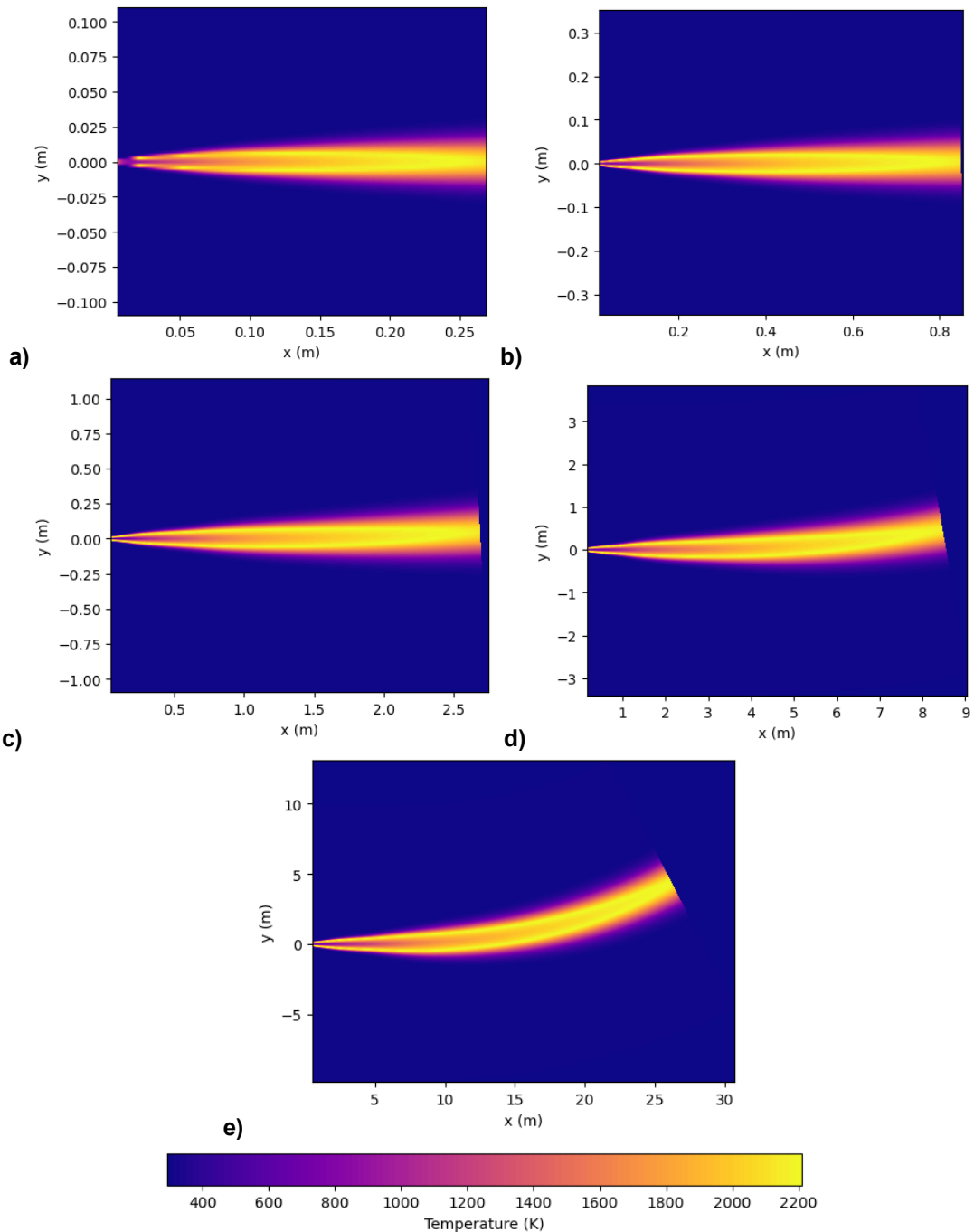


Figure B-15. Temperature contours from a jet fire from a) 0.01%, b) 0.1%, c) 1%, d) 10%, and e) 100% leak directed in the +x direction, for components before the chiller carrying hydrogen at 20°C (68°F) and 900 bar (13,053 psi).

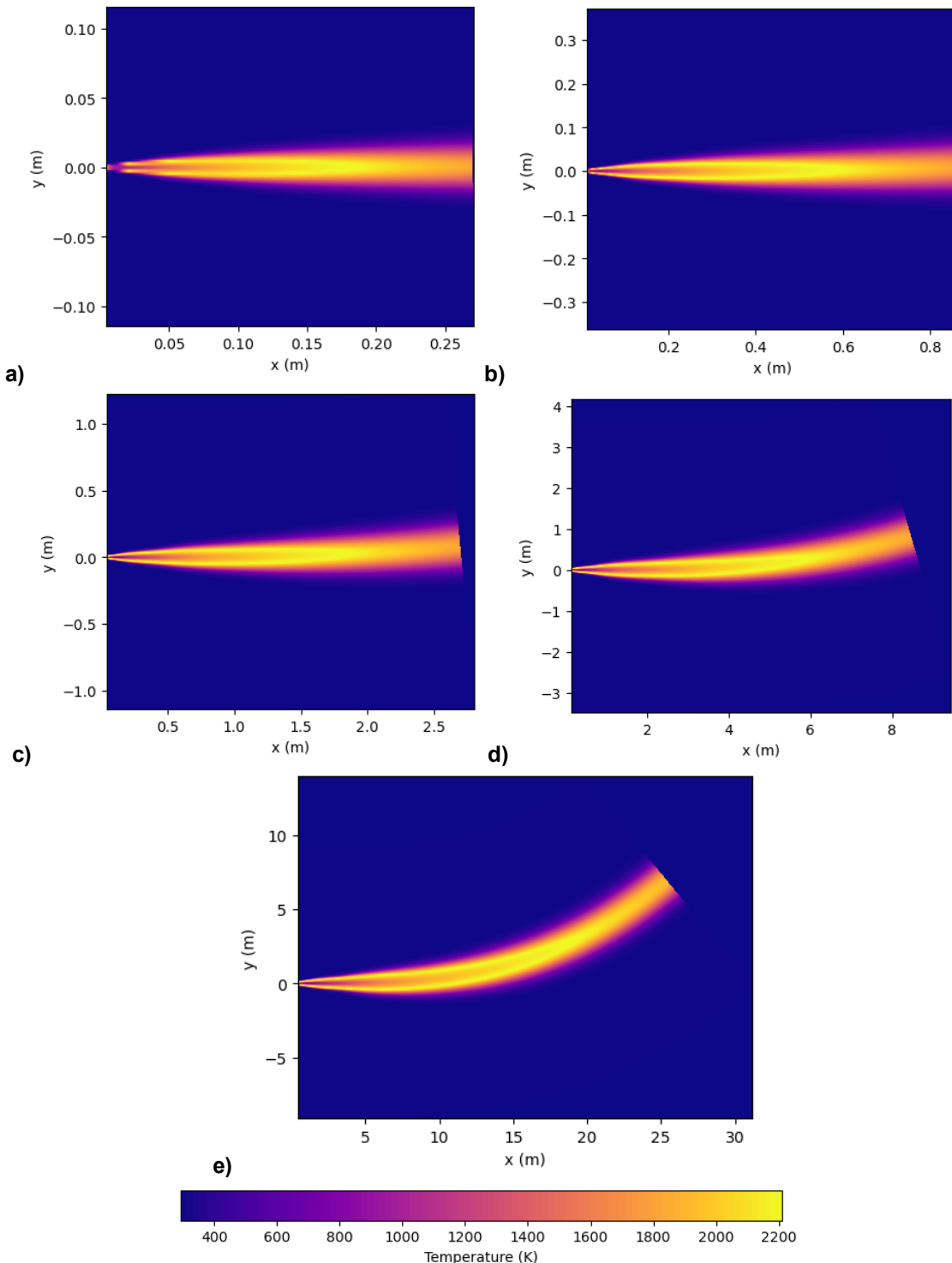


Figure B-16. Temperature contours from a jet fire from a) 0.01%, b) 0.1%, c) 1%, d) 10%, and e) 100% leak directed in the +x direction, for components after the chiller carrying hydrogen at -40°F and 700 bar (10,153 psi).

B.2. Explosion Consequences

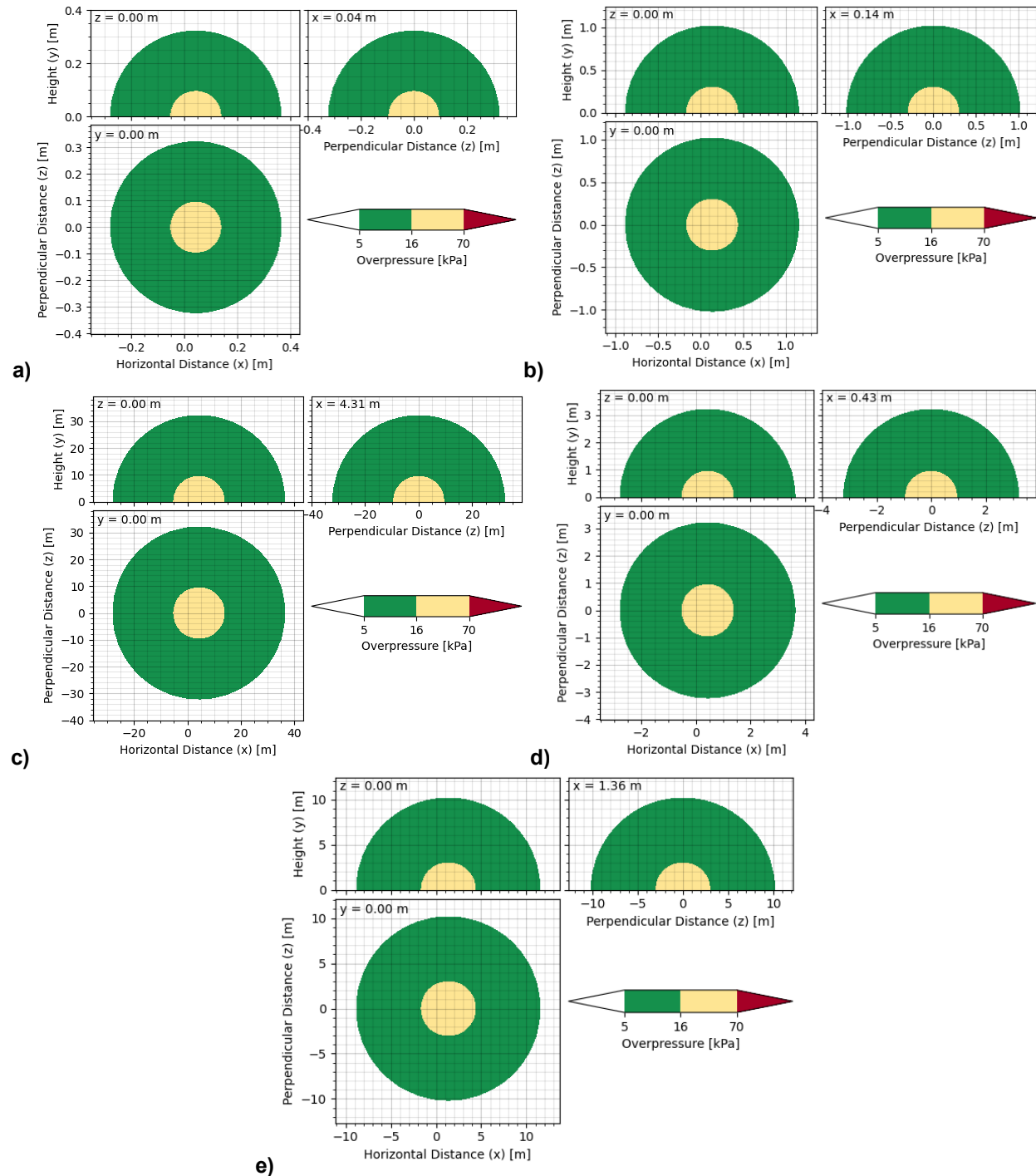


Figure B-17. Overpressure contours from an explosive event from a) 0.01%, b) 0.1%, c) 1%, d) 10%, and e) 100% leak directed in the +x direction, for components before the chiller carrying hydrogen at 20°C (68°F) and 900 bar (13,053 psi). x values are in the direction of the leak, z values are perpendicular to the leak, and y values correspond to height.

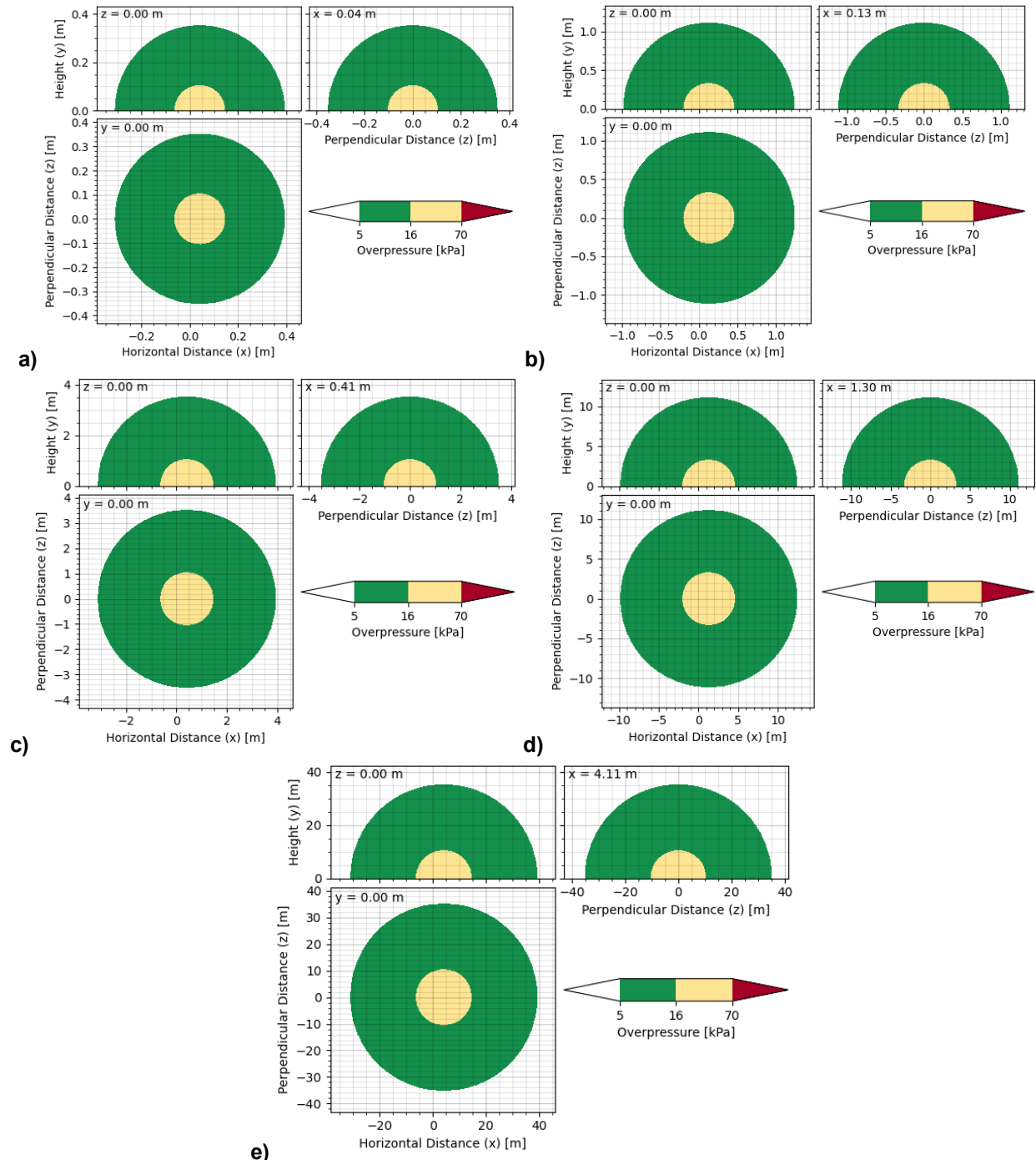


Figure B-18. Overpressure contours from an explosive event from a) 0.01%, b) 0.1%, c) 1%, d) 10%, and e) 100% leak directed in the +x direction, for components after the chiller carrying hydrogen at -40°C (-40°F) and 700 bar (10,153 psi). x values are in the direction of the leak, z values are perpendicular to the leak, and y values correspond to height.

DISTRIBUTION

Email—Internal

Name	Org.	Sandia Email Address
Kristin Hertz	8367	klhertz@sandia.gov
Brian Ehrhart	8854	bdehrha@sandia.gov
Chris LaFleur	8854	aclafle@sandia.gov
Melissa Louie	8854	mlouie@sandia.gov
Marina Miletic	8854	mmileti@sandia.gov
Technical Library	1911	sanddocs@sandia.gov

Email—External

Name	Company Email Address	Company Name
Andrea Caudill	Andrea.Caudill@portofportland.com	Port of Portland
Laura Hill	laura.hill@ee.doe.gov	DOE HFTO
Neha Rustagi	neha.rustagi@ee.doe.gov	DOE HFTO
Arun Veeramany	arun.veeramany@pnnl.gov	Pacific Northwest National Laboratory

This page left blank



**Sandia
National
Laboratories**

Sandia National Laboratories is a multimission laboratory managed and operated by National Technology & Engineering Solutions of Sandia LLC, a wholly owned subsidiary of Honeywell International Inc. for the U.S. Department of Energy's National Nuclear Security Administration under contract DE-NA0003525.